



ENVIRONMENTAL CHEMISTRY OF HYDRAZINE

**Beverly A. Sullivan, B. Patrick Sullivan, John M. Bowen,
Matthew Monroe, Patricia J.S. Colberg, Norbert Swoboda-Colberg,
James T. Markwiese**

**University of Wyoming
Department of Chemistry
Room 409, Physical Sciences Bldg
Laramie WY 82071-4137**

**ENVIRONICS DIRECTORATE
139 Barnes Drive, Suite 2
Tyndall AFB FL 32403-5323**

April 1996

Final Technical Report for Period March 1996 - December 1996

Approved for public release; distribution unlimited.

19961125 161

DTIC QUALITY INSPECTED-3

**AIR FORCE MATERIEL COMMAND
TYNDALL AIR FORCE BASE, FLORIDA 32403-5323**

**ARMSTRONG
LABORATORY**

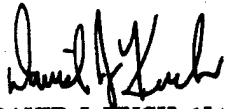
NOTICES

This report was prepared as an account of work sponsored by an agency of the United States Government. Neither the United States Government nor any agency thereof, nor any employees, nor any of their contractors, subcontractors, nor their employees, make any warranty, expressed or implied, or assume any legal liability or responsibility for the accuracy, completeness, or usefulness or any privately owned rights. Reference herein to any specific commercial process, or service by trade name, trademark, manufacturer, or otherwise does not necessarily constitute or imply its endorsement, recommendation, or favoring by the United States Government or any agency, contractor, or subcontractor thereof. The views and opinions of the authors expressed herein do not necessarily state or reflect those of the United States Government or any agency, contractor, or subcontractor thereof.

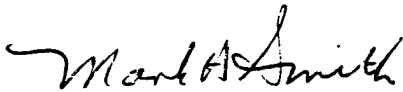
When Government drawings, specifications, or other data are used for any purpose other than in connection with a definitely Government-related procurement, the United States Government incurs no responsibility or any obligations, whatsoever. The fact that the Government may have formulated or in any way supplied the said drawings, specifications, or other data, is not to be regarded by implication, or otherwise in any manner construed, as licensing the holder or any other person or corporation; or as conveying any rights or permission to manufacture, use, or sell any patented invention that may in any way be related thereto.

This technical report has been reviewed by the Public Affairs Office (PA) and is releasable to the National Technical Information Service (NTIS) where it will be available to the general public, including foreign nationals.

This report has been reviewed and is approved for publication.



DAVID J. RUCH, 1Lt, USAF
Project Manager



MARK H. SMITH, Major, USAF, BSC
Chief, Site Remediation

| REPORT DOCUMENTATION PAGE | | | Form Approved OMB No. 0704-0188 | |
|--|---|---|---|--|
| Public reporting burden for this collection of information is estimated to average 1 hour per response, including the time for reviewing instructions, searching existing data sources, gathering and maintaining the data needed, and completing and reviewing the collection of information. Send comments regarding this burden estimate or any other aspect of this collection of information, including suggestions for reducing this burden, to Washington Headquarters Services, Directorate for Information Operations and Reports, 1215 Jefferson Davis Highway, Suite 1204, Arlington, VA 22202-4302, and to the Office of Management and Budget, Paperwork Reduction Project (0704-0188), Washington, DC 20503. | | | | |
| 1. AGENCY USE ONLY (Leave blank) | | 2. REPORT DATE April 1996 | | 3. REPORT TYPE AND DATES COVERED Final Report 1March96-31December96 |
| 4. TITLE AND SUBTITLE Environmental Chemistry of Hydrazine | | | 5. FUNDING NUMBERS C:F08635-93-C-0020 | |
| 6. AUTHOR(S): Beverly A. Sullivan, B. Patrick Sullivan, John M. Bowen, Matthew Monroe, Patricia J. S. Colberg, Norbert Swoboda-Colberg, and James T. Markwiese | | | | |
| 7. PERFORMING ORGANIZATION NAMES(S) AND ADDRESS(ES) University of Wyoming Department of Chemistry Room 409, Physical Sciences Bldg. Laramie, WY 82071-4137 | | | 8. PERFORMING ORGANIZATION REPORT NUMBER | |
| 9. SPONSORING/MONITORING AGENCY NAME(S) AND ADDRESS(ES) AL/EQW-OL 139 Barnes Drive, Suite 2 Tyndall AFB FL 32403-5323 | | | 10. SPONSORING/MONITORING AGENCY REPORT NUMBER Final Report AL/EQ-TR-1996-0004 | |
| 11. SUPPLEMENTARY NOTES Availability of This Report Is Specified on Reverse of Front Cover. AL/EQW Project Officer: Lt David J. Kuch (904) 283-6170 DSN 523-6170 | | | | |
| 12a. DISTRIBUTION/AVAILABILITY STATEMENT This technical report has been reviewed by the Public Affairs Office (PA) and is releasable to the National Technical Information Service (NTIS) where it will be available to the general public, including foreign nationals. | | | 12b. DISTRIBUTION CODE B | |
| 13. ABSTRACT (Maximum 200 words) In order to develop an effective hydrazine remediation technique, the environmental fate and transport of its breakdown products must be identified and quantified. Hydrazine and methyl hydrazine auto-oxidation were studied in the presence of colloidal hematite, a common soil mineral. It was found that auto-oxidation in the presence of the hematite was attenuated when compared to auto-oxidation in water only. This indicates that the interaction between the hydrazines and the hematite in some way protects the hydrazines. The specific interaction between the hydrazines and hematite was investigated using fourier transform infrared spectroscopy using attenuated total reflectance sampling (FTIR-ATR) enabling direct spectral analysis of the interaction without the interference of chemical diluents such as potassium bromide, which are used in more common FTIR methods. These analyses indicated that the interaction is probably due to electrostatic interactions, including hydrogen bonding between the hydrazines and the oxygens, or the first hydration spheres, on the hematite. It was found that the interaction changes with time, and that the interaction is stable to heating, and appear to have a long lifetime, indicating a strong final interaction. Similar results were found when the FTIR-ATR was also used to analyze the interaction of the hydrazines with common clay minerals. | | | | |
| 14. SUBJECT TERMS Hydrazine, Unsymmetrical-dimethylhydrazine (UDMH), monomethylhydrazine (MMH), aeroxine-50, amine, environmental, decomposition, chemistry, soil, groundwater | | | 15. NUMBER OF PAGES 60 | |
| | | | 16. PRICE CODE | |
| 17. SECURITY CLASSIFICATION OF REPORT Unclassified | 18. SECURITY CLASSIFICATION OF REPORT Unclassified | 19. SECURITY CLASSIFICATION OF REPORT Unclassified | 20. LIMITATION OF ABSTRACT UL | |

PREFACE

This report was prepared by University of Wyoming, Department of Chemistry, Room 409, Physical Sciences Bldg., Laramie, WY 82071-4137, USAF Contract No. F08635-93-C-0020, for the Armstrong Laboratory Environics Directorate (AL/EQ), 139 Barnes Drive, Suite 2, Tyndall Air Force Base, Florida 32403-5319.

This final report describes the research conducted to gain a "real world" understanding of the environmental fate of spilled hydrazine fuels. Previous studies verified that hydrazine auto-oxidizes rapidly when exposed to the atmosphere. However, studies concerning the resultant products of the auto-oxidative reaction were lacking. The hydrazine environmental decomposition products of must be identified and quantified in order to provide scientists and engineers a target for the remediation process. This research will allow for the successful development of an inexpensive and environmentally conscious hydrazine remediation/disposal methodology in the field.

The work was performed between March 1995 and December 1995. The AL/EQW project officer was Lt David Kuch.

EXECUTIVE SUMMARY

Hydrazine and methyl hydrazine autoxidation were studied in the presence of colloidal hematite, a common soil mineral. The reaction was followed colorimetrically and analyzed using sorption isotherms. It was found that autoxidation in the presence of the hematite was attenuated when compared to autoxidation in water only. This indicates that the interaction between the hydrazines and the hematite in some way protects the hydrazines. Environmental implications of this finding include enhanced transport of the compounds through the groundwater with the colloidal hematite as a vector, and increased residence times in the environment.

The specific interaction between the hydrazines and hematite was investigated using fourier transform infrared spectroscopy using attenuated total reflectance sampling (FTIR-ATR) enabling direct spectral analysis of the interaction without the interference of chemical diluents such as potassium bromide, which are used in more common FTIR methods. These analyses indicated that the interaction is probably due to electrostatic interactions, including hydrogen bonding between the hydrazines and the oxygens, or the first hydration spheres, on the hematite. It was found that the interaction changes with time, and that the interaction is stable to heating, and appear to have a long lifetime, indicating a strong final interaction. Similar results were found when the FTIR-ATR was also used to analyze the interaction of the hydrazines with common clay minerals.

Finally, the toxicity of hydrazines on soil microflora indicate that in the absence of hematite or clay minerals, that the autoxidation of the hydrazines is rapid enough that the microbes were only exposed to harmless end products. No evidence of the stimulation of microbial growth in the

presence of the hydrazines was found, but evidence indicates that hydrazine is toxic to sulfur reducing soil bacteria.

TABLE OF CONTENTS

| | |
|---|-----|
| Section I | |
| Introduction..... | 1. |
| A. Objective | 1. |
| B. Background | 1. |
| C. Scope | 3. |
| Section II | |
| Experimental Section | 5. |
| A. Materials | 5. |
| B. Instrumentation | 6. |
| C. Methods | 6. |
| D. Toxicity Studies Performed Under Aerobic Conditions | 11. |
| E. Toxicity Studies Performed Under Anaerobic Conditions | 12. |
| Section III | |
| Results and Discussion | 14. |
| A. Effect of Hematite on Hydrazine (NH_2NH_2) Autoxidation | 14. |
| B. Isotherm Study of the Hydrazine/Hematite Interaction | 17. |
| C. Adsorption Behavior of Hydrazine on Hematite by ATR-FTIR Spectroscopy..... | 19. |
| 1. The use of Infrared Analysis on Environmental Samples | 19. |
| 2. Analysis of the Hydrazine-Hematite Interaction | 21. |
| D. Adsorption Behavior of Methylhydrazine on Hematite by ATR-FTIR Spectroscopy | 30. |
| E. Interactions of Hydrazines with Clay Minerals | 33. |
| F. Adsorption Behavior of Hydrazines on Clay Minerals by ATR-FTIR Spectroscopy | 36. |
| G. Oxidation of Dimethylhydrazines as Studied by Gas Chromatography and Mass Spectrometry..... | 45. |
| H. Biological Studies | 49. |
| 1. Effect of Hydrazine and Substituted Hydrazines on Microbial Respiration in Uncontaminated Soils..... | 49. |
| 2. Effect of Hydrazine on Bacterial Sulfate Reduction | 52. |
| Section IV | |
| Conclusions | 54. |
| References | 58. |

LIST OF FIGURES

| | | |
|------------|--|-----|
| Figure 1. | Measurements of the autoxidation of hydrazine with and without hematite..... | 15. |
| Figure 2. | Sorption isotherm showing the interaction between hydrazine and hematite. The surface binding constant and interaction parameter from the Frumppkin equation indicate a strong interaction between the colloid surface and the hydrazine as well as a repulsive interaction between the sorbates..... | 18. |
| Figure 3. | Common vibrational modes for hydrazine. The wavenumbers shown indicate the approximate regions that these modes are found in..... | 20. |
| Figure 4. | Interaction of hydrazine on hematite with time by ATR-FTIR. The cell was not opened between scans..... | 22. |
| Figure 5. | Comparison of FTIR spectra of hydrazine in the vapor phase, A. and in the liquid phase, B. The differences in the positions of the NH stretches indicate hydrogen bonding..... | 25. |
| Figure 6. | Spectra of hydrazine interactions showing evidence for the presence of hydrazinium ion on the surface of hematite. A. Hematite vacuum dried on the ATR cell surface and with water on the surface. B. Hydrazine vapor interacting with the hydrated hematite surface. The 2954 and 2635cm ⁻¹ bands indicate hydrazinium. C. Hydrazine vapor interaction with the vacuum dried surface..... | 28. |
| Figure 7. | FTIR spectra of methyl hydrazine on hematite taken with time..... | 31. |
| Figure 8. | Structural diagrams of clay minerals from Theng (21)..... | 34 |
| Figure 9. | ATR-FTIR spectrum of Georgia kaolin clay KGa-2 showing mineral band positions. | 37 |
| Figure 10. | Spectra of the hydrazine-kaolin interaction with time..... | 38 |
| Figure 11. | Spectra of the interaction of hydrazine with poorly crystallized kaolin with time. Spectra were taken every 20 minutes. Initial spectrum was taken at the 20 minute mark..... | 40 |

| | | |
|------------|---|-----|
| Figure 12. | Differences in vapor deposition of hydrazine and addition of hydrazine as an aqueous solution in KGa-2, poorly crystallized kaolin. Spectrum A. Is the hydrazine-kaolin complex made by vapor deposition, and B. Is made by an addition of aqueous solutions of the clay mineral and hydrazine. The major differences in these spectra are in the NH stretch region just above 3000 wavenumbers and the area just below 3000 wavenumbers..... | 41. |
| Figure 13. | Spectra of SWy-1, sodium montmorillonite with hydrazine added as an aqueous solution. The spectra illustrate the course of the loss of water from the sample on the ATR crystal..... | 43. |
| Figure 14. | Sodium montmorillonite, SWy-1 spectra of A. Deposition of hydrazine from an aqueous solution, and B. Deposition of hydrazine vapor on dry clay..... | 44. |
| Figure 15. | Spectra of hydrazine-calcium montmorillonite prepared from an aqueous solution compared with that prepared by the deposition of hydrazine vapor on dry montmorillonite. The spectrum of pure liquid hydrazine appears at the bottom. Different shifts of the hydrazine bands may indicate a different interaction. The spectra of the calcium montmorillonite has been subtracted out in each case..... | 46. |
| Figure 16. | Gas chromatogram of UDMH, decomposition products and the solvent..... | 48. |
| Figure 17. | Production of CO ₂ by soil microorganisms with 5 or 50 mg/L of hydrazine, methyl hydrazine and phenyl hydrazine or no added hydrazines (controls). The data plotted represent the mean results of triplicate biometer flasks. L = 5 mg/L; H = 50mg/L..... | 50 |
| Figure 18. | Production of CO ₂ by soil microorganisms with 100 and 200 mg/L of hydrazine, methyl hydrazine and phenyl hydrazine or no added hydrazines (controls). The data plotted represent the mean results of triplicate biometer flasks. L = 100 mg/L; H = 200 mg/L..... | 51. |
| Figure 19. | Hydrazine inhibition of sulfate reduction in the <i>D. desulfuricans</i> . Data represent the mean sulfate values obtained from quadruplicate microcosms..... | 53 |

LIST OF TABLES

| | | |
|----------|--|-----|
| Table 1. | Infrared Spectral Assignments for Hydrazine, Methyl Hydrazine and Their Hematite Adsorbates..... | 24. |
| Table 2. | Partial Infrared Spectral Data for Hydrazinium Ion and the Hydrazine/Hematite Adsorbate..... | 29. |
| Table 3. | Infrared Spectral Properties of Methyl Hydrazine and its Hematite Interactions..... | 32. |

SECTION I

INTRODUCTION

A. OBJECTIVE

The objective of this study was to determine the effect of various common minerals on the autoxidation reaction of three hydrazine compounds. The lifetime of the hydrazine compounds in various water samples has been measured, however, the mechanisms of these reactions in the presence of various mineral surfaces has not been thoroughly investigated. For this paper, the environmental fate and autoxidation of three hydrazine compounds in water and the effect on these reactions of specific and well defined high surface area minerals was studied. In order to determine the fate of these environmentally sensitive compounds in the "real world," the specific intermolecular interactions between the hydrazine compounds and mineral surfaces that give rise to the chemical behavior governing the fate of the hydrazines must be well understood. This requires that the autoxidation reaction for these compounds in relation to the minerals be studied with only one mineral at a time instead of with an entire, ill defined mixture. This study includes the measurement of the autoxidation of three hydrazine compounds in the presence of colloidal hematite. In addition, a spectral analysis of this interaction, and the interaction of these compounds with common, well defined clay minerals was done. The effect of biological degradation on the three hydrazine compounds was also studied.

B. BACKGROUND

Because the United States Air Force uses hydrazines as fuel components, it is desirable to understand the fundamental chemistry of hydrazines in the environment. For the purposes of this

work the hydrazines under consideration are, hydrazine itself, methyl hydrazine (MH), N,N-dimethyl hydrazine (UDMH) and aeroxine-50 (AZ-50). Hydrazine, and its analogs, methyl hydrazine and N,N dimethyl hydrazine, have been used as high energy density aviation fuels, or fuel additives for nearly 50 years. They are also used in other industrial settings such as for boiler antioxidants. These compounds, which are polar and quite soluble in water, are also strong reducing agents, and are all considered toxic (1). Because of their water solubility and widespread industrial and avionic use, the opportunity for spills during storage or transportation creates a potential for environmental contamination (2). As a further complication, hydrazine compounds are also known to autoxidize in the presence of oxygen through a series of reaction steps, which in some cases can be surface-catalyzed (3-9). Without catalysis, the autoxidation can be very slow (10) but can also be catalyzed with metals widely present in soils such as Fe^{3+} , Cu^{2+} and Mn^{3+} . In these reactions, the metal cations are reduced to lower oxidation states by the hydrazines, and apparently cycle back to the higher oxidation state by reaction with atmospheric oxygen. In the case of iron-containing montmorillonitic clays or humic materials, hydrazine will reduce the Fe^{3+} and has been shown to complex with it (11).

One nearly ubiquitous source of the Fe(III) in the environment is colloiddally dispersed hematite ($\alpha\text{-Fe}_2\text{O}_3$), an example of an oxyhydroxide. Colloidal compounds are also known to be reactive and to have large surface areas which may offer more contact of the iron sites in the mineral with natural waters contaminated with hydrazines. It is also known that colloidal particles can be carried with groundwater, in which case the contaminants attached to them can be spread slowly

through the environment. Because of these processes, it is of interest to determine what effect hematite and other naturally occurring minerals may have on the fate and transport of hydrazines.

If hydrazines are accidentally discharged, their chemistry in both aqueous (surface and ground water) and soils comes into play. We have studied the chemistry of the hydrazines in water, and in the presence of well-defined soil constituents. The importance of well defined chemical systems cannot be overstated since the "real-world" applicability of this research will come only if the critical variables are isolated, understood, and then manipulated to achieve effective chemical or biological remediation.

Previous work has identified the interactions and some of the chemistry of hydrazines with naturally occurring soil constituents, including clays and other oxide minerals. In our work, we have examined environmental hydrazine interactions in the following areas:

1. Interactions of hydrazines with hematite: physical and chemical studies
2. Interactions of hydrazines with clays: physical studies
3. Oxidation reactions in aqueous solutions with emphasis on product identity
4. Biological studies

C. SCOPE

In addition to work aimed at understanding the fundamental chemical behavior of hydrazines, we performed microbiological experiments to complement the reactivity work. We had initially anticipated studies which would assess the potential for hydrazine to be used by bacteria as an

electron donor or as a sole source of nitrogen; however, the finding that hydrazine autoxidized to form nitrogen gas rather than nitrate (NO_3^-) made such experiments moot. Also experiments originally proposed to assess the potential for microbial transformation of the carbon containing methyl and phenyl substituted hydrazines were not performed, since soils with a history of hydrazine exposure were not available, and the period of performance was too short to complete our own exposure experiments.

The primary objectives of the modified microbiological work were to assess the toxicity of hydrazines to microorganisms under both aerobic and anaerobic conditions. The rationale for the work was based on reports that hydrazines may be toxic to mammalian cells (Sullivan, personal communication); any demonstrated toxicity of hydrazines to microbes would not bode well for their biological removal in the environment. Toxicity assays were performed (12) with naturally occurring microorganisms living in uncontaminated soils under aerobic conditions (hydrazine, methyl hydrazine and phenyl hydrazine) and (13) with a pure culture of sulfate-reducing bacteria (*Desulfovibrio desulfuricans*) grown under anaerobic conditions (hydrazine only).

This report will discuss the results in the above areas and summarize the environmental significance of our findings.

SECTION II

EXPERIMENTAL SECTION

A. MATERIALS

The hydrazine and methyl hydrazine used were purchased from Aldrich Chemical Company. They were 98% pure compounds and were used after distillation and after successful comparison of their infrared spectra against the literature (14). Vanillin was also purchased from Aldrich Chemical Co., and was used without further preparation. All other reagents used in the vanillin colorimetric detection for hydrazine (15), including sulfuric acid and ethanol were drawn from stock reagents purchased from reputable chemical supply houses.

Colloidal hematite was prepared from Fe(III) chloride using the preparation described by Penners and Koopal (16). After production, colloid particle size was determined to be between 600 and 1800 nm by photon correlation spectroscopy depending on the preparation.

Clay minerals were purchased from the Source Clay Repository at the University of Missouri-Columbia, and included SWy-1 sodium montmorillonite from Crook, County, Wyoming, SAz-1 or Cheto calcium montmorillonite from Apache County, Arizona, KGa-1b, well crystallized kaolin from Washington County, Georgia, and KGa-2 poorly crystallized kaolin from Warren County, Georgia. These clays were used without further purification.

B. INSTRUMENTATION.

UV-Visible absorption spectra used in the determination of the amount of unbound hydrazine in the sorption isotherm study were obtained with a Hewlett-Packard 8452 spectrometer. Fourier Transform Infrared (FTIR) spectra were obtained using a Bomem B-102 FTIR instrument, at 4 cm^{-1} resolution, and a Graseby-Specac ATR assembly. The instrument was controlled by and spectral manipulation was achieved with the use of Bomem-Grams 386 software manufactured by Galactic Industries Corporation. Peak positions were obtained from the infrared spectra using the Bomem-Grams 386 software standard peak pick routine which picks the three points of maximum intensity. Because of this, some uncertainty in the band positions we have listed occur and so this paper discusses only the band shifts greater than 4 cm^{-1} .

Gas chromatography and gas chromatography-mass spectrometry experiments utilized distilled water, prepared in-house using a millipore apparatus and various solvents such as diethyl ether, methanol which were taken from stock materials without further purification. All solvents used from house stocks were purchased from reputable chemical supply companies.

C. METHODS.

All of the infrared spectra used in this study were obtained using Attenuated Total Reflectance-FTIR (ATR-FTIR). This method of obtaining infrared spectra utilizes an infrared transparent crystal, (ZnSe in this case) where the incident IR beam is transmitted into a beveled face of the crystal. The beam is internally reflected against the upper and lower surface of the crystal several times before leaving the crystal and passing on to the detector of the FTIR instrument. At the

points of reflection in the crystal, the electric vector of the infrared light is able to interact with any sample coated on the surface of the crystal, thus producing an infrared spectrum of the sample. This makes a convenient method for the infrared analysis of environmental samples.

For the ATR-FTIR analysis of sorption interactions (17), reference spectra of hematite deposited from an aqueous suspension on the ZnSe-ATR crystal were obtained against an air-background spectrum. The co-added background spectrum was then subtracted from the co-added spectra of interest to produce the FTIR spectrum observed. This procedure allows the spectrum of the unaltered hematite to be observed. Upon reaction with the hydrazines, the new spectral traces include bands from both the hematite and the hydrazine-hematite adsorbates. Alternatively, to observe only the hydrazine-hematite interaction, the spectrum of deposited, unreactive hematite was used as the background spectrum. Any changes in the hematite spectrum would appear as negative or second derivative-like absorptions.

Reaction of the hydrazine with hematite was done by spreading 5-10 μL of the hydrazine compound on the cap or lid of the ATR assembly and tightly sealing the lid over the ATR crystal. This allowed the hydrazine vapor to come in contact with the deposited hematite for the amount of time chosen for the experiment. In some cases, it was necessary to obtain FTIR spectra of the changes in the hydrazine-hematite spectrum with time. In these cases, the Bomen-Grams 386 kinetics software routine, which allows kinetic changes to be monitored, was used. During these timed runs, the lid of the ATR assembly was not opened.

Adsorption isotherms were obtained for the analysis of the effects of hematite on the autoxidation of hydrazine. For these experiments, solutions of hematite were exposed to hydrazine, and the autoxidation was measured, using a colorimetric assay for free hydrazine in solution. Non buffered and buffered aqueous solutions of 5×10^{-1} to 2×10^{-3} M hematite in total iron, as assayed by acidic digestion and thiocyanate colorimetry, were used. The reactions were run in batch in a darkened reaction vessel. At given times from 15 minutes to up to 72 hours, aliquots of the reaction solution were extracted in triplicate, filtered with 0.22 μ L Millipore filters to remove the hydrazine adsorbed to colloidal hematite material, and were placed in three scintillation vials. At this point the solutions were acidified and a vanillin solution was added according to the procedure of Sulbha and Gupta (15). After the color forming reaction was completed, the samples were serially assayed for unbound hydrazine at times ranging from 15 minutes to 72 hours using the vanillin reaction, and quantitated colorimetrically at 400 nm. An ϵ_{max} of $3.249 \times 10^{-6} \text{ M}^{-1}\text{cm}^{-1}$ was determined for use in this study (15).

The effect of pH on the reaction was initially explored in two separate experiments at a pH of 4.0 and pH 7.0. In these initial experiments, the pH was adjusted immediately before the vanillin assay. In further experiments, tris(hydroxymethyl)aminomethane (TRIS) buffer was used because it is widely held to be a non interacting buffer system which will not precipitate cations such as calcium or magnesium. When this buffer is used as a mixture of TRIS base and TRIS HCl at a final concentration of 0.05 M, it is most effective in its ability to maintain pH values between pH 7 to 9. TRIS buffers were prepared at pH 7.0 and pH 8.5 and were then used to prepare colloidal hematite to a concentration of 1.125×10^{-3} M, and hydrazine to a concentration of 3.5×10^{-5} M.

In addition, the effect of aggregation of the colloidal hematite and its effect on the autoxidation of hydrazine was studied at two concentrations of colloidal hematite with a median particle size of 750 nm. The concentrations for colloidal hematite used were 1.125×10^{-3} M and 1.125×10^{-4} M and were incubated with and without 3.5×10^{-5} M hydrazine in both water and in TRIS buffer at a pH of 8.5 for 60 minutes. The absorbance from light scattering off the colloids was monitored spectrophotometrically at 600, 700, and 750 nm at 1-minute intervals.

The analyses of the interactions between clay minerals and the hydrazines using ATR-FTIR were similar to those with hematite. Two methods were used for this study, the first involving vapor deposition and the second involving liquid deposition. In the first method, the clay minerals were made into a thin slurry with a minimal amount of water and added to the ATR cell where the mixture was allowed to dry. At this point, the cell was placed in the FTIR and a spectrum of the thin film of the clay mineral was taken, either as a spectrum against an air background to obtain the spectrum of the minerals themselves, or as a background spectrum. For the vapor deposition spectra of the hydrazine-clay mineral sorbate, between 10 and 50 μ L of a hydrazine compound was placed on the interior surface of the cell lid which was then closed and sealed over the sample on the cell. This allowed the vapor of the hydrazine compound to contact the clay mineral. The second method involved the addition of an aqueous hydrazine solution to the hydrated clay mineral to determine the differences involved in the mode of deposition. For this method, two mixtures were made up for each clay mineral. In each case, 0.2 grams of clay mineral were added to 2 mL of distilled water. In one of these mixtures, 0.1 mL hydrazine was also added and mixed. For the

ATR-FTIR analysis, the mixture without the added hydrazine was used as the baseline spectrum, followed by the spectrum of the mixture with the added hydrazine. In all cases, the mixture was added to the ATR cell, and allowed to dry before FTIR analysis.

For the oxidation studies, both the GC and GC-MS instruments were based on the Hewlett-Packard 5890 Series II gas chromatograph. The available detector for the GC was a flame-ionization detector (FID). Dimethyl hydrazine was used since an FID might not effectively detect the final products of the oxidation reaction. Both instruments used a HP-5 Cross linked 5% PH ME Silicone capillary column, with a 0.25 μm film thickness. For preliminary studies, methyl hydrazine was added to distilled water as a 10% by volume mixture which was stirred in a reactor consisting of a large stoppered flask filled to the halfway mark to allow for adequate oxygen equilibration. One-milliliter samples were taken at 10-minute intervals and 0.2 μL were injected through the HP gas chromatograph. These preliminary studies revealed that the water peak eluted very close to that of the dimethyl hydrazine peak, although some peaks were also observed at longer reaction times and at later retention times. This presented problems with the GC-MS analysis of the methyl hydrazine parent peak, and those initial degradation products of similar molecular weights and elution times as the GC-MS used has incorporated safety procedures which shut off the MS detector during the time period around which the solvent peak elutes to protect it from being destroyed. This allowed only peaks with elution times after the detector safety time period to be analyzed by GC-MS. To address these problems, another method was developed to analyze for these products based on head space analysis. Here, the reactor sample was made up, and 1-mL samples were taken as before. After the aqueous samples were taken, they were added

to 0.5-mL diethyl ether in a miniature separation flask. After extraction, a small amount of the ether solution was placed in a sealed vial and allowed to equilibrate at 25° C for 5 minutes. After the equilibration time, 0.5 μ L of the vapor over the solution was extracted and injected into the GC.

D. TOXICITY STUDIES PERFORMED UNDER AEROBIC CONDITIONS

The toxicity of hydrazine, methyl hydrazine and phenyl hydrazine (Sigma, St. Louis, MO) to soil microorganisms was assessed in biometer flasks (Bellco, Vineland, NJ) containing organic-rich garden soil and hydrazine concentrations ranging from 5-200 mg/L. Among treatments, comparisons of CO₂ evolution (μ mol/g soil) over time gave an indication of relative toxicity of the individual hydrazines. Each experimental treatment consisted of three replicate biometer flasks at each hydrazine concentration. Each experiment had its own set of killed controls.

Biometer flasks (250 mL) were used to quantify respiration by the soil microbial community. Flasks were stored in the dark to prevent loss of CO₂ due to photosynthetic activity. The soil matrix consisted of 40 g (sieved to 2 mm) of garden soil that was rich in organic material and 15 mL of deionized water with or without (i.e., controls) the respective hydrazines. Evolved CO₂ was trapped in the flask sidearm which contained 10 mL of 0.02N NaOH. NaOH was periodically removed with a syringe and titrated until colorless with 0.02N HCl. The volume of acid required to neutralize the NaOH was recorded. Fresh NaOH was replaced in the sidearm with a syringe, and the flasks were returned to a dark cabinet until the next sampling.

Rates of CO₂ production for each replicate flask (n=3) in each treatment (n=7) were calculated for the lower concentrations of hydrazines (5 and 50 mg/L). CO₂ production was linear over time. The slopes for each treatment were compared using a one-way analysis of variance at $\alpha = 0.05$. Rates of CO₂ production for the higher concentrations of hydrazines (100 and 200 mg/L) were more characteristic of logarithmic bacterial growth. Treatments (n=7) were compared with total CO₂ produced (n=3) per treatment in a one-way analysis of variance $\alpha = 0.05$.

E. TOXICITY STUDIES PERFORMED UNDER ANAEROBIC CONDITIONS

The toxicity of hydrazine to a pure culture of *Desulfovibrio desulfuricans* was assessed at concentrations of 5, 50 and 100 mg/L with four replicates/treatment. Toxicity was assessed in terms of inhibition of the sulfate reduction. A treatment without added hydrazine (also in quadruplicate) served as the control.

Standard anaerobic techniques were used throughout (12). Gases used in media preparation were passed through a column of heated copper filings to remove traces of oxygen. All transfers and culture samplings were performed in an anaerobic chamber (Coy, Grass Lake, MI) with a N₂/H₂ (95/5%) atmosphere. Gases inside the chamber were continuously recirculated through a freshly activated platinum catalyst to remove any traces of oxygen.

Desulfovibrio desulfuricans (ATCC 7757), a sulfate-reducing bacterium, was grown in a mineral salts medium with sodium lactate (20 mM) as the carbon source and sodium sulfate (20 mM) as the sulfate source (13). Ten mL of media were bubbled with N₂ for 6 minutes in 25-mL glass test

tubes (Bellco Glass, Inc.). Each tube of sulfidogenic medium was sealed with a thick butyl rubber stopper and an aluminum crimp seal. The anaerobic medium was autoclaved at 121° C for 15 minutes. The pH of the autoclaved medium was about 6.8. Cultures were started with a standardized inoculum. All transfers and sampling were performed with a sterile needle and syringe for each treatment so that there was no possibility of transferring bacteria between the tubes.

Stock solutions of hydrazine were prepared using degassed deionized water (bubbled with oxygen-free N₂ for 45 min). The concentration of hydrazine sulfate (Sigma, St. Louis, MO) in each stock solution was such that the addition of 1 mL to each culture yielded final solution concentrations of 5, 50 and 100 mg/L hydrazine for a total liquid volume of 12 mL. The control cultures (no added hydrazine) received 1 mL of anaerobic deionized water. Hydrazine stock solutions were not autoclaved before introduction into the sterile anaerobic media; their addition did not significantly affect media pH.

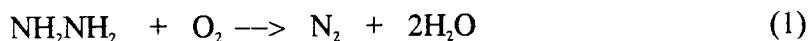
Sulfate in the medium was quantified using a Dionex Model DX-100 Ion Chromatograph equipped with an anion-guard column, AS4A separator column and suppressor. Sulfate standards ranged from 0 to 30 mM sulfate. A dilute carbonate buffer was used to elute sulfate. Each experimental replicate was sampled twice for sulfate for each time interval and the average value was recorded.

SECTION III

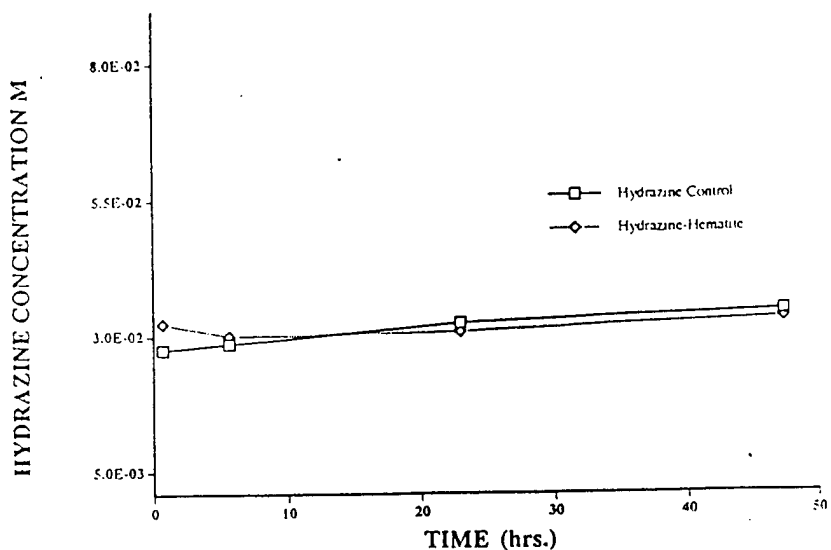
RESULTS AND DISCUSSION

A. EFFECT OF HEMATITE ON HYDRAZINE (NH₂NH₂) AUTOXIDATION

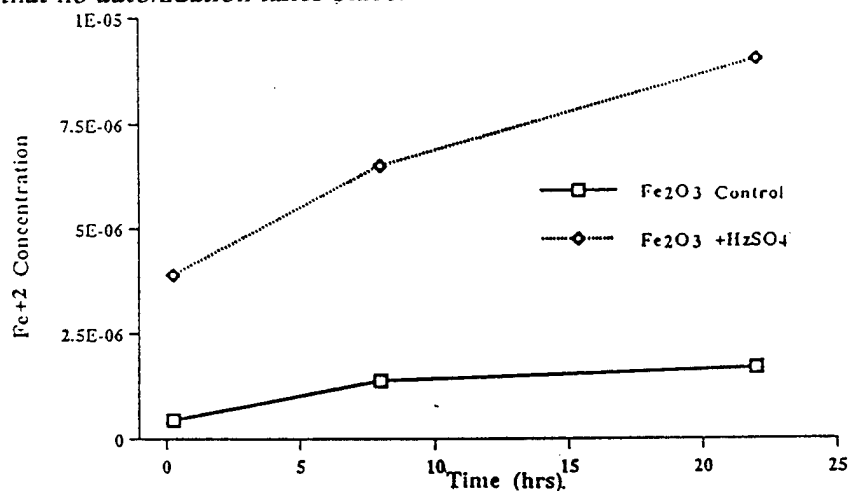
The effects of hematite on the autoxidation of the parent hydrazine was determined using hematite colloids of sizes between 600 to 1800 nm, using both unbuffered and buffered solutions. Under these conditions, the autoxidation of hydrazine is well known (Equation (1.)) (2), (6-10), and these experiments were designed to determine the effect of the presence of the colloidal iron mineral.



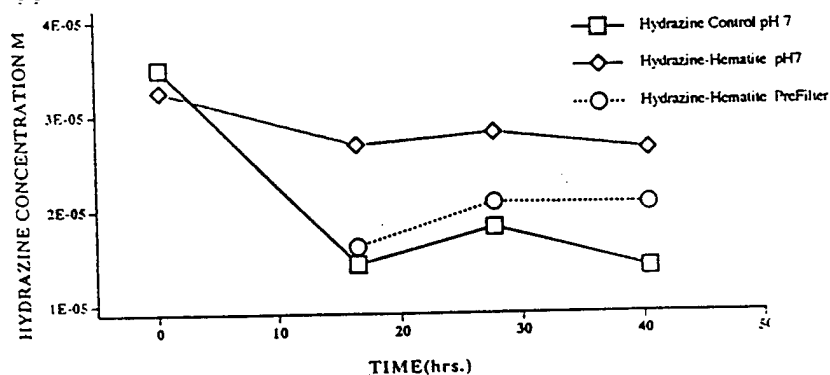
Fe⁺³_(aq) under a variety of pH conditions is known to catalyze the autoxidation of hydrazine, itself being reduced to Fe⁺², but the oxidation in the presence of hematite, a common iron containing substituent in groundwater, has not been studied. In the initial experiments at low pH, it was determined that the autoxidation of hydrazine was negligible. At pH 4.0, no autoxidation was observed at a hydrazine concentration of 3.0 x 10⁻² M, either in the presence or absence of the colloidal hematite, as shown in Figure 1a. That this reaction proceeded slowly at a higher hydrazine concentration, since Iron (II) was detected, as seen in Figure 1b. At pH 7.0 and at a hydrazine concentration of 3.5 x 10⁻⁵ M, hydrazine autoxidation was observed, however, in the presence of colloidal hematite this reaction was found to be substantially attenuated. These experiments were conducted so that the vanillin assay was equilibrated with the hematite and then removed by filtration after the assay (see experimental). The assumption was that the total



a. Experiment with hydrazine with and without presence of hematite at pH 4.0 indicating that no autoxidation takes place.



b. Slow autoxidation at lower pH occurs at higher hydrazine concentrations as seen by the appearance of reduced iron leached from the hematite structure.



c. Autoxidation of hydrazine in the presence of hematite was attenuated as compared to the control at pH 7.0.

Figure 1.

Measurements of the autoxidation of hydrazine with and without hematite.

hydrazine concentration remaining was measured by the assay. If the identical experiment was performed, but with filtering the hematite colloid from the solution prior to the vanillin assay, a significantly lower hydrazine concentration was found than in the post filtered experiments. This result strongly implicates an adsorption process, where hydrazine binding to the colloidal hematite is dominant, as can be seen in Figure 1c.

In a related series of experiments, TRIS buffer was used to maintain the solutions at a given pH. When pH was controlled in the presence of the TRIS buffer at both pH 7 and pH 8.5, similar effects were seen in the control and in the filtered samples as shown in Figure 1c, where the pH was adjusted at the time that the reaction was sampled. However, quantitatively, autoxidation was diminished in the buffered samples when compared to the unbuffered samples, again providing evidence for adsorption of hydrazine to hematite rather than an enhancement of autoxidation.

A significant result was that aggregation and precipitation of the hydrazine-exposed colloid occurred over time under a variety of experimental conditions. Aggregation occurred as a function of concentration. At concentrations below about 10^{-3} M total iron, slow (over hours) aggregation or precipitation occurred, with or without added hydrazine. However, at concentrations above this limit, aggregation was detected within about two minutes. Precipitation also was seen in about 30 minutes for hematite in the presence of TRIS buffer. In an aqueous solution without the buffer, the colloid remained unaggregated. Based on these data, adsorption isotherms with hydrazine and the colloidal hematite were researched at a total concentration of Fe(III) of 10^{-4} M.

B. ISOTHERM STUDY OF THE HYDRAZINE/HEMATITE INTERACTION

From the above results, retardation of hydrazine autoxidation by hematite colloids at 10^{-4} M Fe(III) implies a strong chemical or physical interaction between hydrazine and the hematite colloid surface. The result of an isotherm experiment to determine the hydrazine-surface interaction is shown in Figure 2. The data were fit to the Frumppkin isotherm (18), which below in Equation (2).

$$K_{eq}[\text{NH}_2\text{NH}_2] = (\theta/(1-\theta))\exp(a\theta) \quad (2)$$

Here the values of K_{eq} , known as the surface binding constant and a , the interaction parameter were found to be 7.8×10^3 and -0.8 respectively. In the equation, θ , the surface coverage, was determined by difference as discussed in the experimental section. These values indicate a tightly bound form of hydrazine on the surface of the colloidal hematite, and a repulsive interaction between the adsorbates. As a consequence of this result, the mechanism of the surface interaction was explored by infrared spectroscopy.

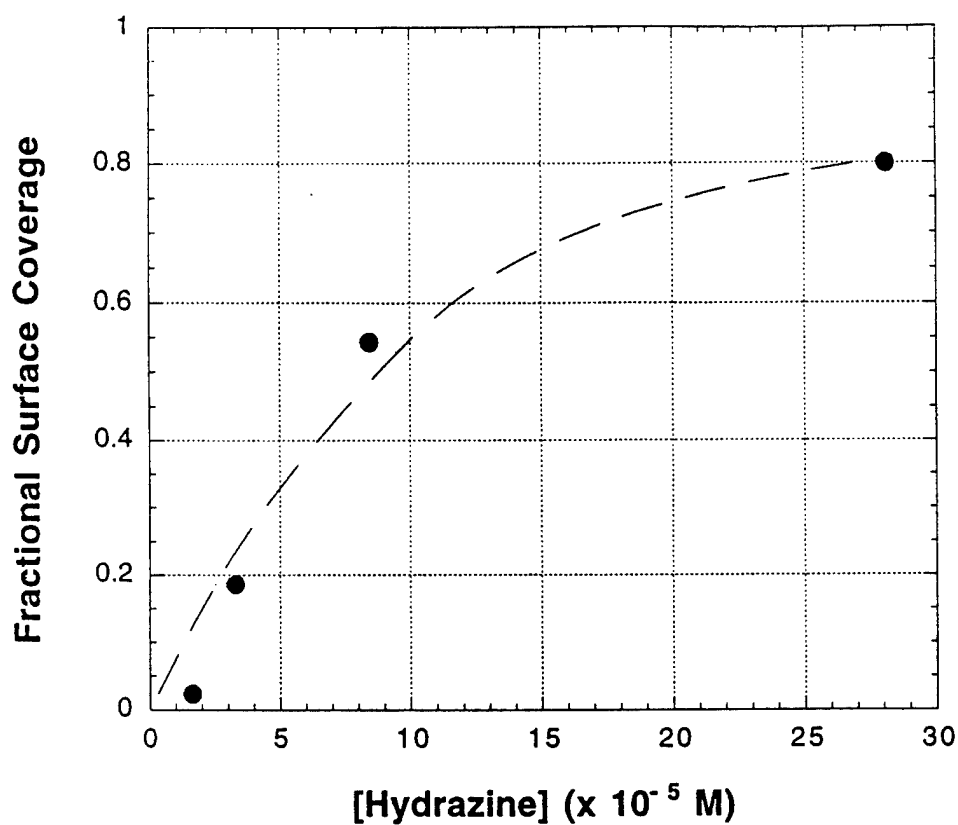


Figure 2.

Sorption isotherm showing the interaction between hydrazine and hematite. The surface binding constant and interaction parameter from the Frumppkin equation indicate a strong interaction between the colloid surface and the hydrazine as well as a repulsive interaction between the sorbates.

C. ADSORPTION BEHAVIOR OF HYDRAZINE ON HEMATITE BY ATR-FTIR SPECTROSCOPY

1. The Use of Infrared Analysis of Environmental Samples

Infrared spectroscopy deals with the interaction of infrared radiation with matter. The subregion of the infrared electromagnetic spectrum that was used in this study is called the mid-infrared region which extends from about 200 to 4000 cm^{-1} . In this region, nearly all molecules will absorb energy from the infrared radiation into their vibrational modes. The multiplicity of the possible vibrational transitions found in most molecules can cause the resultant infrared spectrum to be quite complex. Because of these complex spectra in this IR region, which is divided into the "group frequency" 4000-1250 cm^{-1} region, and the "fingerprint" region, 1250-400 cm^{-1} , this spectroscopic technique is especially suited to qualitative analysis. Further, each band in these regions corresponds to a particular vibrational mode of the molecule being analyzed so that detailed analysis of these bands are of great assistance in the determination of the molecular structure of a compound. These vibrational modes are visible in the IR spectrum if the bond associated with that vibrational mode can absorb the radiation at a particular wavenumber (radiation frequency which is proportional to the energy of the radiation), such that the dipole moment of that bond changes with the vibrational motion. These vibrational motions, depending on the structure of the molecule, can be more or less independent of vibrational motions of the rest of the molecule, and will appear in different regions of the mid-infrared spectrum. They can be tentatively identified by comparison with a "correlation chart", found in almost any spectroscopy text. These molecular vibrational motions include stretches, bends, wags, rocks, etc. as is illustrated below in Figure 3. using hydrazine as an example.

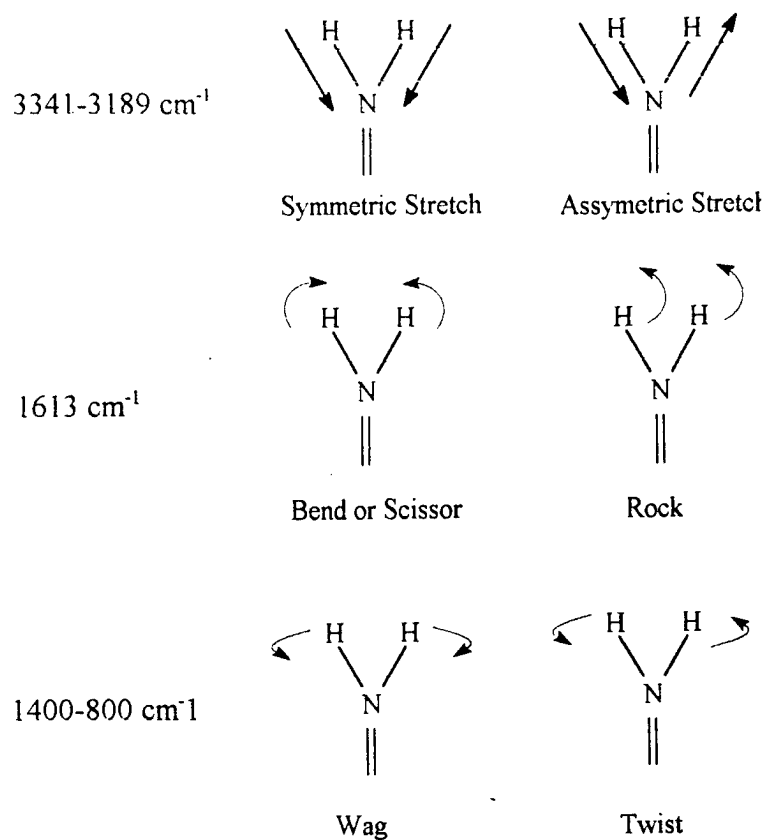


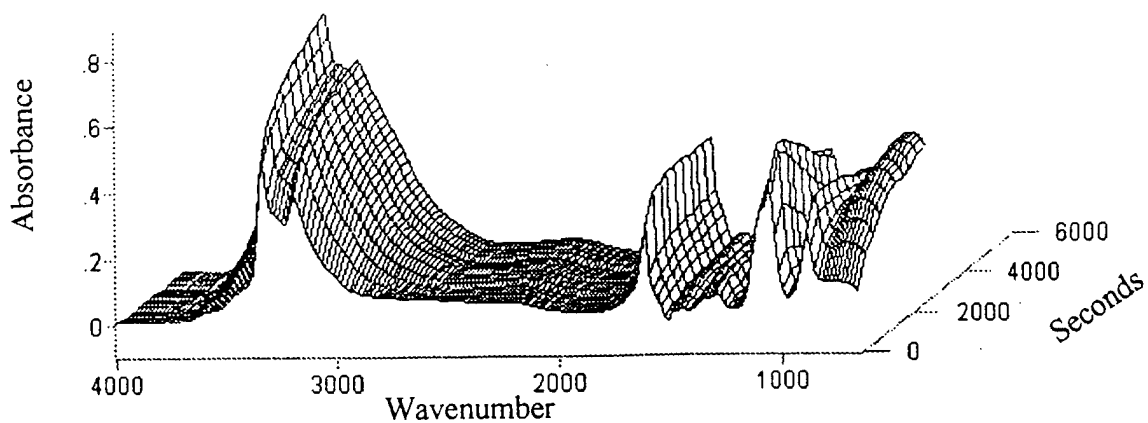
Figure 3.

Common vibrational modes for hydrazine. The wavenumbers shown indicate the approximate regions that these modes are found in.

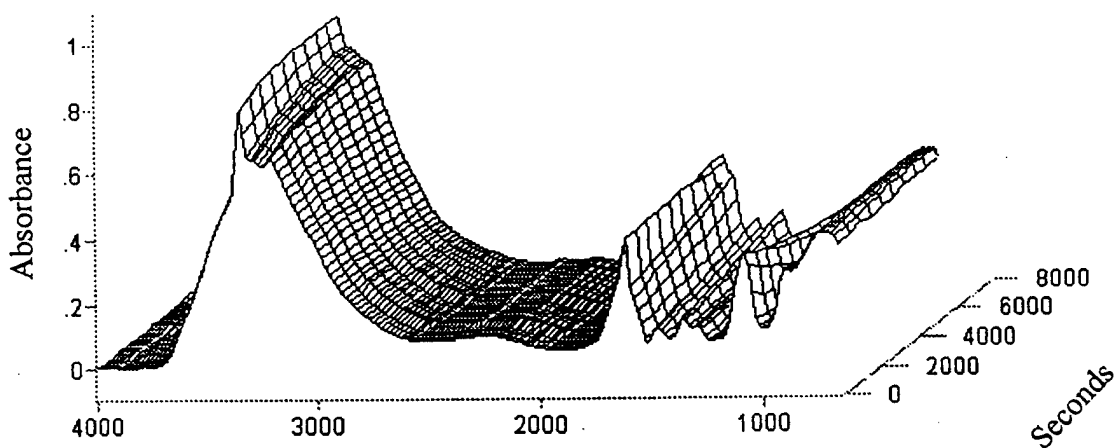
In addition to the qualitative characteristics of the infrared bands, these bands are affected by changes in their environment. For instance, if an N-H bond in hydrazine is perturbed by an interaction such as hydrogen bonding to another negative center, such as a surface oxygen on hematite, the position of that N-H bond in the infrared spectrum will change. In this case, the band position will be shifted to lower wavenumber in proportion to the strength of the hydrogen bond. This can be seen in the position of the N-H stretches of hydrazine in the vapor phase when compared to hydrazine in the liquid phase where more hydrogen bonding takes place. Other bonds in the molecule, and the vibrational bands associated with them, will also be affected in proportion to their distance on the molecule from the interaction. From the analysis of these band shifts, the type of interaction of the original molecule with another molecule, or in this case the surface of the hematite colloid, can be deduced making infrared analysis of the interactions between pollutant compounds and surfaces a very powerful tool for environmental analysis. The infrared analysis of the interaction between the hydrazines and the hematite surface examined in this study is based on these observations.

2. Analysis of the Hydrazine-Hematite Interaction

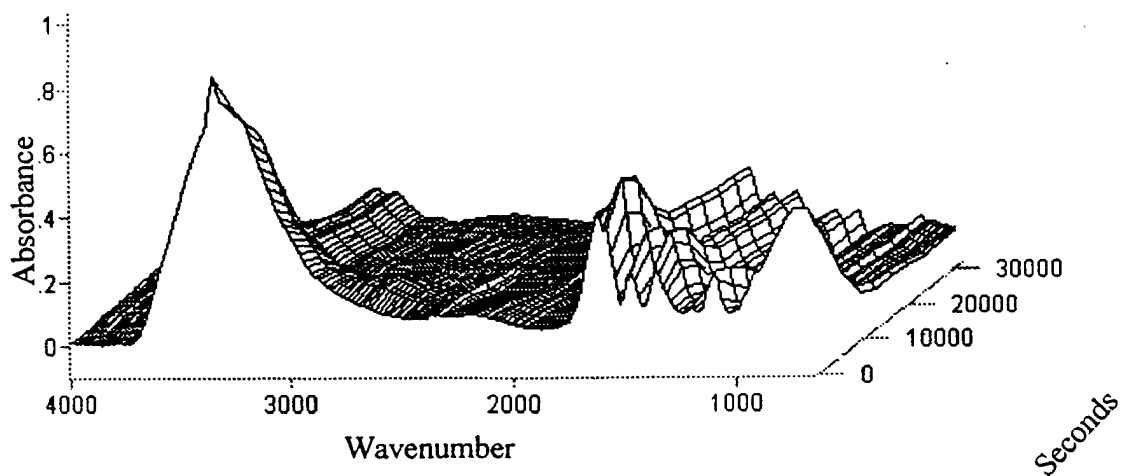
The adsorption behavior of vapor phase hydrazine on the hematite was initially assumed to be subject only to equilibrium and kinetic restraints. Therefore, preliminary experiments were designed to determine the adsorption behavior of vapor phase hydrazine on dried hematite using an ATR cell. In later experiments, ATR spectra of aqueous solutions followed by spectral subtraction were used to determine the identity of suspected species in the solution deposition.



A Time from 0.0 to 45 minutes exposure to hydrazine. 5 min between runs.



B. Exposure time from 45 minutes to 145 minutes. 10 minutes between runs.



C. Exposure time from 145 minutes to 745 minutes. 60 minutes between runs.

Figure 4.

Interaction of hydrazine on hematite with time by ATR-FTIR. The cell was not opened between scans.

In both cases, the spectral bands associated with the hydrazine-hematite interaction appear to be similar. In our experiments, hematite which had been dried onto the surface of the enclosed ATR cell, was exposed to hydrazine vapor, and followed by ATR-FTIR with time. The ATR cell remained closed throughout the total of 12.4 hours for a typical experiment, and results of a typical experiment can be seen in Figure 4. For these, the FTIR spectrum of the dried hematite was used as the background so that the mineral bands are not seen. The resultant spectra are therefore comprised only of the bands associated with vapor phase hydrazine and hydrazine-hematite complex. It is apparent from these spectra that changes in relative intensity, and some band shifting, occur during the course of the experiment. This is seen in Figure 4a. which depicts the first ten spectra, taken every 5-minutes. The initial spectrum, shown in the foreground, is similar to that of pure-vapor phase hydrazine (seen in Figure 4a. as differing only in the position of some of the bands) (see Table 1). During the course of this experiment, the intensity of the hydrazine spectra grow in intensity as the vapor-phase hydrazine reacts with the hematite on the surface of the ATR cell. A comparison of the N-H stretch band (the IR absorption bands corresponding to the stretching mode of the N-H moiety) positions from the initial interaction, (listed as 0 min in Table 1), with those of the vapor spectrum show that these bands at the start of the experiment appear to be shifted from their positions in the vapor-phase by 8 and possible 3 cm^{-1} to lower wavenumber or energy, respectively. If the spectra of vapor-phase and liquid-phase hydrazine are compared, a similar shift to lower wavenumber (Figure 5), 9 cm^{-1} and possible 3 cm^{-1} for the liquid phase is found for the N-H stretches. According to previous work (19), this difference between the positions of the N-H stretches in the vapor and liquid phase indicates hydrogen bonding. In a similar fashion, the differences between the initial spectrum and that of the

TABLE 1. INFRARED SPECTRAL ASSIGNMENTS FOR HYDRAZINE, METHYL
HYDRAZINE AND THEIR HEMATITE ADSORBATES.

Note: The wavenumbers in this study are somewhat different from those found in the references due to the differences in instrumentation. In order to be consistent, the pure vapor spectra of hydrazine and methyl hydrazine were run on the instrument used in this study and the position of the bands found were compared against those of the complexes.

| ASSIGNMENT | HYDRAZINE VAPOR | COMPLEXES | | |
|-------------------------|-----------------|-----------|--------|-------------|
| | | 0 Min | 45 Min | 745 min |
| NH str | 3341s | 3336s | 3347s | 3336s |
| NH str | 3189s | 3187s | 3203s | 3172s |
| NH ₂ scissor | 1613m | 1612m | 1613m | 1588m |
| ? | 1470m | 1484w | 1478w | 1474m |
| ? | 1442sh | 1452w | 1447w | ** |
| NH ₂ wag | 1351m | 1350sh | 1351m | 1372m |
| NH ₂ wag, sh | 1291sh | 1288sh | 1285sh | ** |
| NN str, sh | 1101sh | 1101sh | 1121sh | 1216w |
| NH ₂ str | 1065s | 1056m | 1080m | 1193m |
| NH ₂ wag | 895w | 887m | 895w | 951 or 811w |

** not seen

sh = shoulder, w = weak, m = medium, s = strong

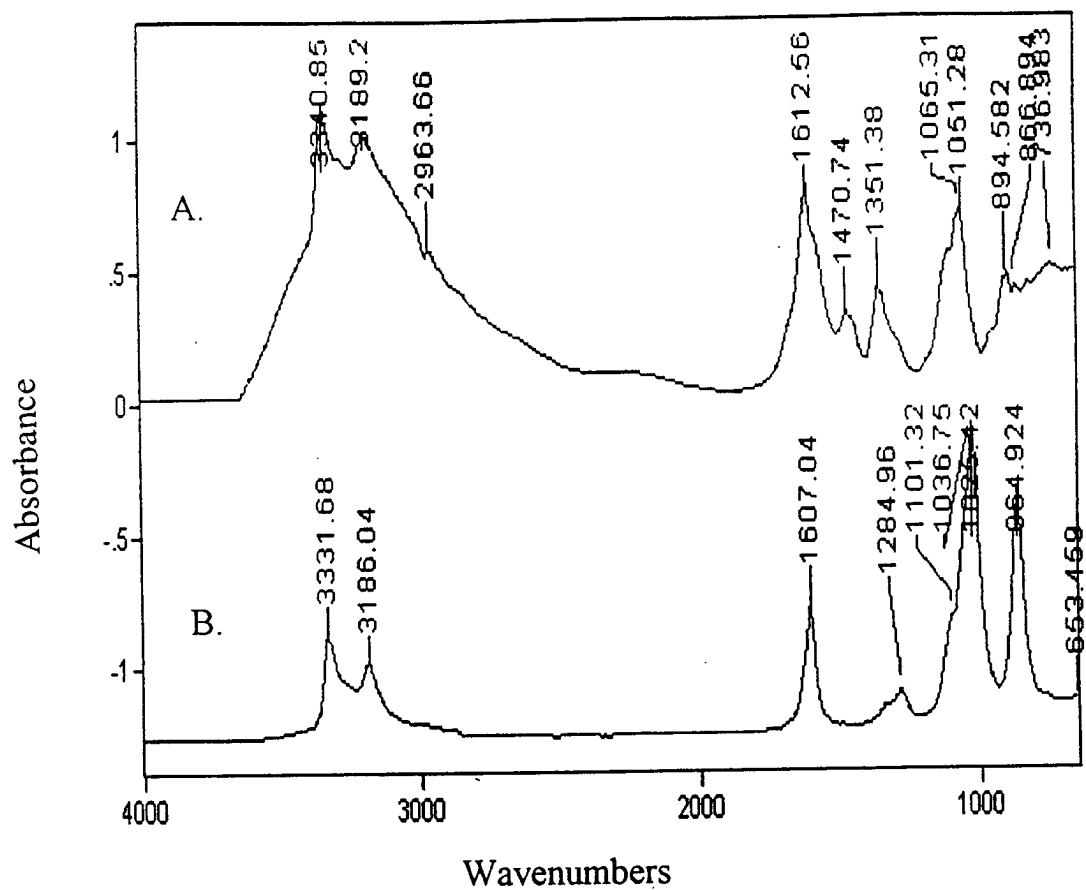


Figure 5.

Comparison of FTIR spectra of hydrazine in the vapor phase, A. and in the liquid phase, B. The changes in the N-H stretches from 3341 and 3189 cm^{-1} in the gas phase to 3331 and 3186 cm^{-1} in the liquid phase indicate hydrogen bonding.

vapor phase hydrazine spectrum reveal a 4 cm^{-1} and possible 2 cm^{-1} shift to lower energy and probably indicates that hydrogen bonding plays an initial role in the interaction between hydrazine and hematite.

As the experiment progressed (Figure 4b.) it was seen that, in addition to the rise in the intensity of the NH stretch bands to a maximum from 45 minutes to 145 minutes, these bands also shift from their initial values of 3336 and 3187 cm^{-1} to higher wavenumber at 3347 and 3214 cm^{-1} , which may indicate that within the first few minutes of exposure a kinetically controlled interaction takes place between the colloidal mineral and the hydrazine. As shown in Figure 4c, another dramatic change occurs in the NH stretch region at around the 5.5-hour mark. At this point, there is a large intensity decrease in, and a concurrent shift of, the N-H stretches to 3213 and 3172 cm^{-1} . In addition, the NH_2 wags (another IR active vibrational mode, see Figure 3) found initially at 1334 cm^{-1} and 1285 cm^{-1} in Fig 3a. are shifted respectively 27 cm^{-1} and 24 cm^{-1} to higher energy or wavenumber at the end of the timed experiment.

The mechanism of interaction between the hydrazine and the hematite appear to be controlled by the amount of water present on the hematite surface. It was hypothesized that in aqueous solution, where the pH is below its pK_a , that hydrazine will abstract a hydrogen from a water molecule to form a hydrazinium ion which can hold either a charge of 1^+ or 2^+ (20-22). In order to test this hypothesis, two further experiments were performed. In the first, hematite was air dried

In the first, hematite was air dried such that the mineral was hydrated (see figure 6a), while in the second, the hematite was dried under vacuum such that little water was available for proton abstraction by hydrazine. When hydrazine vapor was added using the same method as in the previous experiments, it was seen for the hydrated sample at about the 4 hour mark, that bands identifiable as the NH_3^+ stretches described by Glavic (20) at 2944 and 2708 cm^{-1} were easily visible at 2954 and 2635 cm^{-1} with the second band shifted to lower wavenumber presumably due to hydrogen bonding with negative moieties on the hematite surface. In the less hydrated sample, the same bands can be seen as well, but at lower intensity. As the NH_3^+ stretches for hydrazinium 2^+ are listed as weak in intensity in the infrared (20) due to the symmetry of the ion, it is likely that the interaction with the hematite is through the hydrazinium 1^+ ion through either the water molecules of the first hydration sphere on the hematite surface or with the hematite lattice oxygens. Table 2 shows the positions of the bands in the spectral region which we attribute to the hydrazinium ion compared with those found in the hematite colloid.

Upon heating, these bands remained indicating that the interaction is not labile. The bands attributed to dry hematite are also included in the table for comparison. The differences between the bands of the hydrazine sulfate and the adsorbate bands may be attributed to the interaction with the mineral.

After about 45 minutes, a large shift of the N-N stretching band seen initially at 1101 cm^{-1} , and the NH_2 stretching bands at 1065 cm^{-1} are observed to shift to higher energy by around 15-20 cm^{-1} . This shift is consistent with the structure of the hydrazinium ion, where one of the nitrogens is

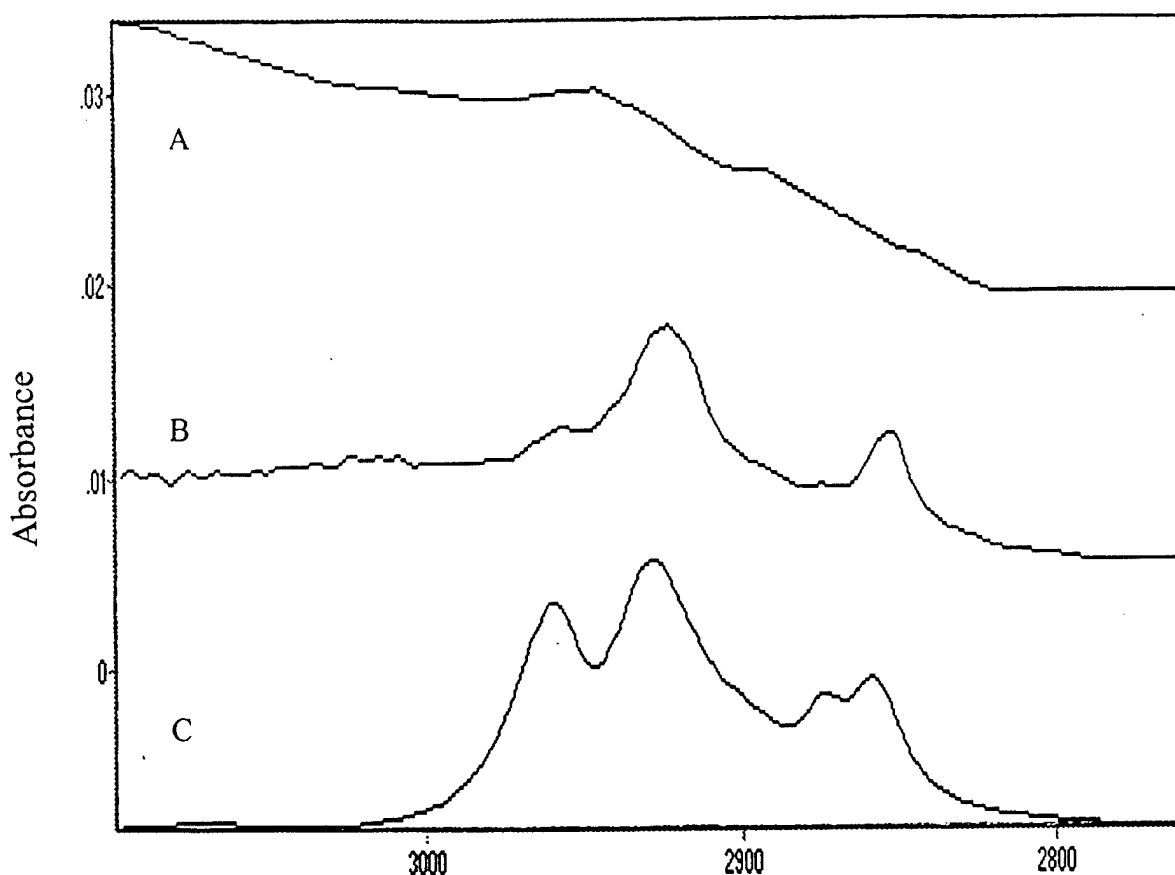


Figure 6.

Spectra of hydrazine interactions showing evidence for the presence of hydrazinium ion on the surface of hematite.

- A. Hematite dried on the ATR cell surface and exposed to hydrazine vapor.
- B. A difference spectrum of hydrazine in an aqueous hematite-TRIS buffer solution at pH 7.0 with the hematite-TRIS spectrum subtracted. This shows the characteristic bands from hydrazinium just below 3000 cm^{-1} .
- C. Hydrazine sulfate evaporated onto the surface of the ATR cell.

TABLE 2. PARTIAL INFRARED SPECTRAL DATA FOR HYDRAZINIUM ION AND THE HYDRAZINE/HEMATITE ADSORBATE

In the NH_3^+ stretch region.

| Hydrazine sulfate | Hydrazine monochloride | Adsorbate | Hematite |
|-------------------|------------------------|-----------|----------|
| 2930w | 2944vs | 2954s | 2944m |
| 2790w | 2708s | ** | 2921m |
| 2590w | 2580s | 2635s | |
| 2100w | | ** | |

** not seen

sh = shoulder, w = weak, m = medium, s = strong, v = very

protonated, this relieving the steric repulsion between the nitrogen lone pairs to some degree. The NH_2 stretch originally at 1065 cm^{-1} can also be seen to increase over the course of the experiment. The final positions of the NH stretches appear at lower energy to the vapor phase by 5 cm^{-1} and 17 cm^{-1} , which may indicate that the adsorbate at the end of the experiment is also undergoing a hydrogen bonding situation with the surface, in addition to the electrostatic surface attraction. A reaction depicting this probable interaction is shown in Equation (3).

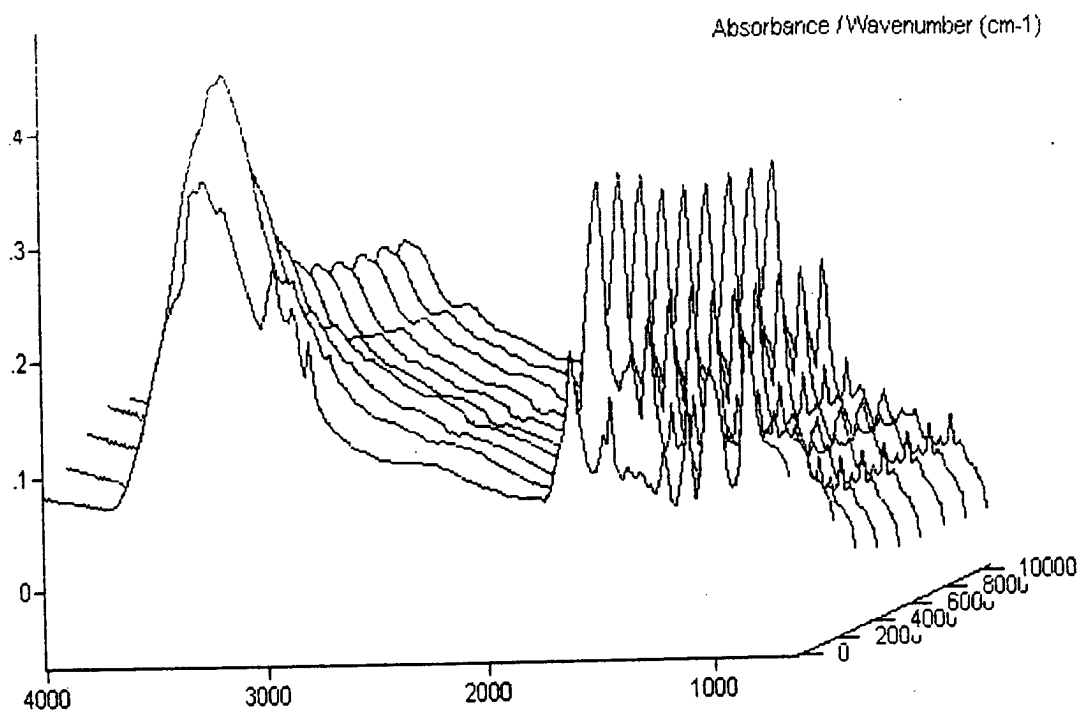
(3)

D. ADSORPTION BEHAVIOR OF METHYLHYDRAZINE ON HEMATITE BY ATR-FTIR SPECTROSCOPY.

A similar series of experiments involved methylhydrazine and hematite. As shown in Figure 7, the spectra of the interaction also changes with time as in the hydrazine-hematite experiment, however all of the changes appear to take place within the first fifty minutes. As can be seen in Figure 7a, substantial change occurs in the NH stretch region. The initial spectrum, seen in the foreground, is very similar to that of methylhydrazine in the vapor phase, and as with the hydrazine-hematite interaction this interaction also grows in intensity, and energy. Ten minutes into the experiment, the NH stretches have shifted from their initial values at 3315, 3256 and 3179 cm^{-1} to 3322, 3266, and 3172 cm^{-1} . After this, the band at 3315 cm^{-1} disappears, and the intensity of the NH stretch region rapidly decreases leaving two bands at 3329 and 3163 cm^{-1} . Unlike the hydrazine interaction, the NH stretch bands of methylhydrazine do not consistently shift to lower energy, indicating that hydrogen bonding may not be the initial interaction between this molecule and the hematite surface.

Unfortunately, in the region between 3000 and 2700 cm^{-1} , where the bands which we attribute to the hydrazinium ion occur, the CH stretches from the single methyl group obscure interpretation. However, an interesting change takes place as the interaction proceeds. In the initial spectrum, the recognizable CH stretch bands in the first or foreground spectrum in Fig. 6a appear in almost the identical positions as that of the gas phase (see Table 3). But within 10 minutes, these bands begin shifting and losing intensity with the band at 2787 cm^{-1} completely disappearing. It is not known

A.



B.

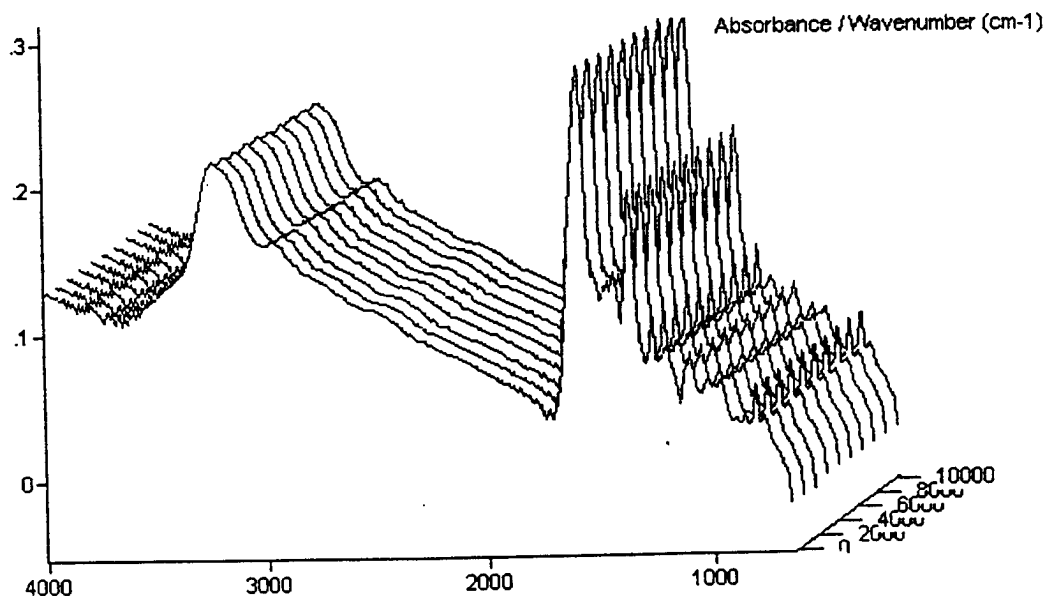


Figure 7.

FTIR spectra of methyl hydrazine on hematite taken with time.

TABLE 3. INFRARED SPECTRAL PROPERTIES OF METHYL HYDRAZINE AND ITS HEMATITE INTERACTIONS

(All figures are in wavenumbers)

| ASSIGNMENT | MHZ VAPOR | COMPLEXES | | |
|----------------|-----------|-----------|---------|---------|
| | | 0 Min | 240 Min | 420 Min |
| NH str | 3317 | 3315 | 3226 | ** |
| NH str | 3265 | 3268 | 3226 | 3228 |
| NH str | 3176 | 3179 | 3167sh | 3161sh |
| CH str | 2971sh | 2972sh | 2971sh | 2972w* |
| | 2939m | 2944m | 2952m | 2953w* |
| | | | 2920w* | 2921w* |
| | 2884wsh | 2892vw* | | |
| | 2859m | 2863w | 2850w* | 2850w* |
| | 2841wsh | 2844wsh* | | |
| | 2783m | 2787w | | |
| NH2 sym deform | 1614m | 1614m | 1588vs | 1589vs |
| CH3 deform | 1478sh | 1478sh | noise | noise |
| | 1444m | 1446m | 1433sh | 1433sh |
| | 1412? | 1414? | | |
| | | 1375w | 1366vs | 1366vs |
| ? | 1307m | 1312w | | |
| | | 1272w | 1268m | 1268m |
| CH3 wag | 1204m | 1208m | 1208w | |
| NH2 wag | 1137? | | | |
| NH deform | 1124sh | 1123wsh | 1119wsh | 1118wsh |
| Skeletal str | 1098m | 1098m | 1098m | 1098m |
| CH3 wag | 958vs | 1000s | 1024w | 1024w |
| | | | 982w | 962w |
| NH2 rock | 886? | ** | ** | ** |
| Skeletal str | 814vs | 832m | 851w | 851w |
| | | | 804m | 804m |
| | | | 760w | 760w |

* may be due to hydrazinium ion

** not seen

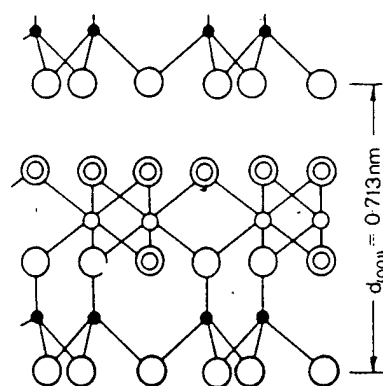
sh = shoulder, w = weak, m = medium, s = strong

whether the new bands are merely shifted CH_3 stretches or are bands attributable to a methyl hydrazinium ion. At lower wavenumber, (between 1600 cm^{-1} to 800 cm^{-1} , in this case) including the bending and wagging areas of the IR spectra, Table 3 shows that little change is observed, other than an unassigned band which appears at 1271 cm^{-1} , and at the CH_3 wag (near 1000 cm^{-1}) which splits into two bands, one at 1021 and the other at 961 cm^{-1} . Also, the skeletal stretch at 832 cm^{-1} apparently splits into three components, which occur at 851 , 804 and 760 cm^{-1} . It is obvious that an interaction occurs with methyl hydrazine and that it impacts the bands associated with the methyl group is apparent. However, it is not certain whether this interaction is through a hydrazinium ion as is postulated with the hydrazine-hematite interaction. These questions need to be answered in a new phase of this study.

E. INTERACTIONS OF HYDRAZINES WITH CLAY MINERALS

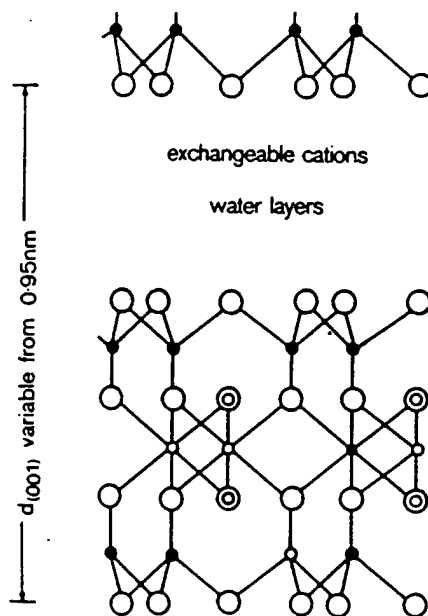
Adsorption of compounds on clay minerals depends on the chemical nature of their exposed surfaces. This is true of 1:1 clays such as kaolinite, or 2:1 clays such as smectites, of which montmorillonite is an example. Adsorption also depends on whether the clay can readily exchange interlamellar cations, or whether reaction occurs with surface constituents (17, 23). Kaolinite clays such as KGa-1b and KGa-2 as well as smectite clays including SAz-1 and SWy-1 were used in this study. The following diagram adapted from Theng (23) (Figure 8a) shows the structure of the kaolinite and montmorillonite clay minerals. The diagram shows parts of two layers of the

Kaolinite



- Key:
- Oxygen
 - ⊙ Hydroxyl
 - Aluminium
 - Silicon

Montmorillonite



- Key:
- Oxygen
 - ⊙ Hydroxyl
 - Aluminium
 - Silicon
 - ⊙ Magnesium, Iron

Figure 8.
Structural diagrams of clay minerals from Theng (21)

clay, which actually consists of a repeating structural motif. Adsorption of hydrazine as the hydrazinium ion can take place by interacting with the hydroxyls bound to the aluminum atoms, or with the oxygens in the silicate layer. This takes place between the layers in the interlamellar space. In order for this kind of sorption to take place, the interlamellar distances must range from 0.05-2 nm: this can additionally enlarge when hydrated. Alternatively, sorption directly to the aluminum atoms exposed on clay edges is another possibility for negatively charged sorbates, or electron pair donors such as the hydrazines. For the montmorillonites, shown in the same diagram, a structural feature is the symmetry in its layering, with only oxygens in the interlamellar spaces. The consequence of this is that montmorillonites are known to bind ions such as Ca^{2+} and Na^{+} into these spaces, providing additional sites for negatively charged, or lone pair donors to bind (i.e., in the coordination sphere of the ion). Potentially positively charged sorbants such as hydrazinium ions also could exchange with the interlamellar cations. Based on this picture, it could be argued that differences in the sorption mechanism of hydrazines on clay minerals could occur between vapor deposition of hydrazine, and sorption of hydrazinium ions from aqueous solution.

In previous work, Moliner and Street (11) determined that hydrazine sorbed to kaolinite, montmorillonite and other soil clay materials, and used a batch reaction method to produce adsorption isotherms. They determined that the primary interactions with hydrazine and the montmorillonite clays took place at below the pK_a of hydrazine (7.96), especially in the case of the sodium montmorillonites. It was postulated that the hydrazinium ion was involved in a simple ion exchange reaction with the interlamellar sodium ions.

F. ADSORPTION BEHAVIOR OF HYDRAZINES ON CLAY MINERALS BY ATR-FTIR SPECTROSCOPY.

In our study, slurries of each of four clay minerals were dried on the ATR cell to create thin films, and the spectra of these were taken over a period of time. These spectra were compared with a hydrazine-clay mineral preparation made from aqueous solution. In the case of the kaolinite clay minerals, the infrared spectra seen in Figure 9 of the clay mineral by itself shows the intense Si-O stretching band at around 1000 cm^{-1} . The region between 1100 cm^{-1} to nearly 3600 cm^{-1} is free of any spectral features. When the clay films are dried, both the well crystallized and the poorly crystallized kaolinites have nearly identical spectra except for minor shifts around the clay mineral bands below 1000 cm^{-1} . When the clay mineral is exposed to hydrazine in the vapor phase, the initial spectrum is very similar to that of vapor phase hydrazine, just as is found in the interaction with hematite (see Figure 10). The spectra in Figure 10a represent the first 200 minutes of the experiment, while those in Figure 10b represent the second 200 minutes of the experiment. These spectra show the vapor phase deposition of hydrazine on KGa-1b, which is a well crystallized kaolin. It can be seen that within the first 20 minutes, the NH stretch bands have shifted from their initial vapor phase values at around 3332 cm^{-1} and 3191 cm^{-1} to final positions around 3270 cm^{-1} and 3182 cm^{-1} . After this 20 minute change, little change occurs in the infrared spectra throughout the balance of the experiment. In this initial period a highly structured OH stretch appears as a narrow band at 3416 cm^{-1} . This band most likely represents highly hydrogen bonded structural hydroxides or water in the interlamellar spaces of the kaolin which has been disturbed by the binding of hydrazine from the vapor phase. During the initial experiment it can be seen that a series of bands at around 3000 cm^{-1} , 2956 cm^{-1} , 2917 cm^{-1} and 2848 cm^{-1} appear and increase in

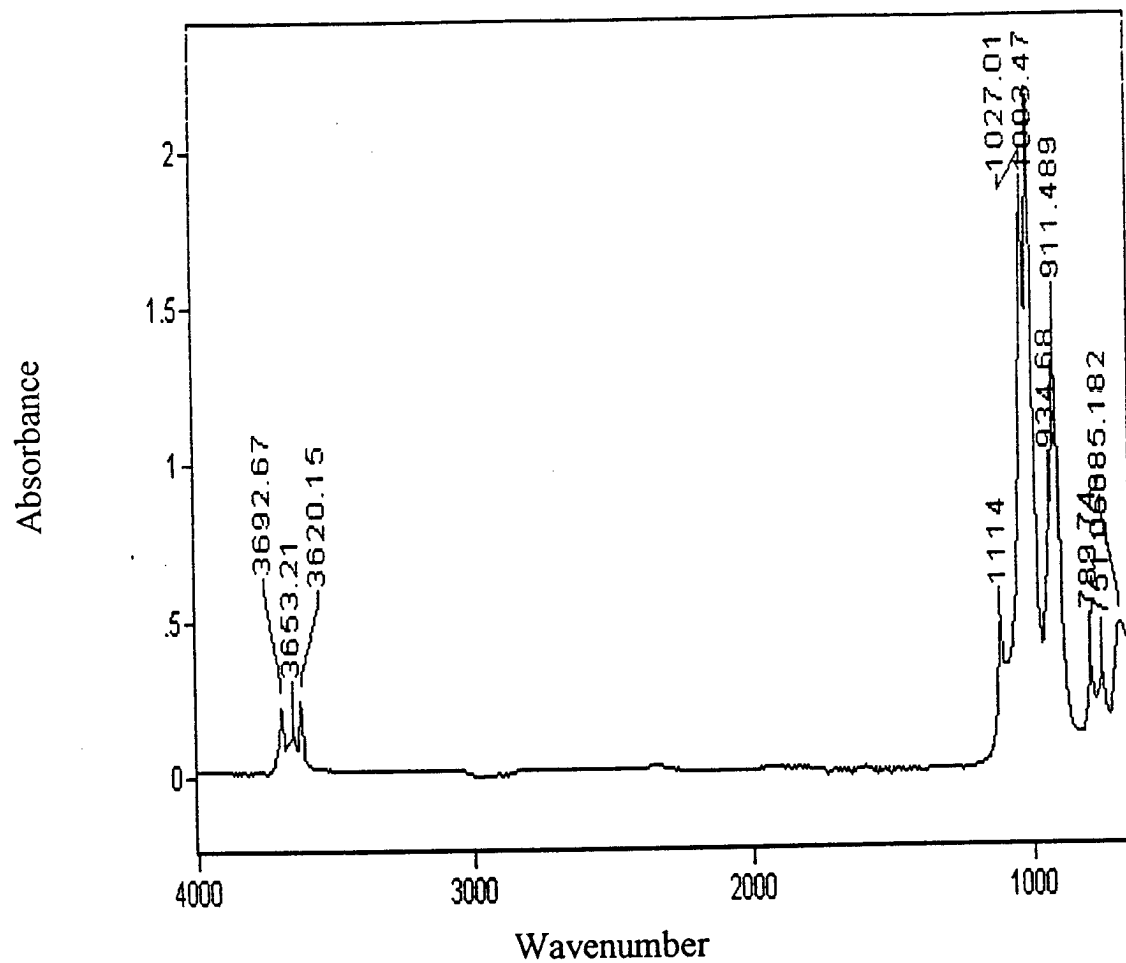
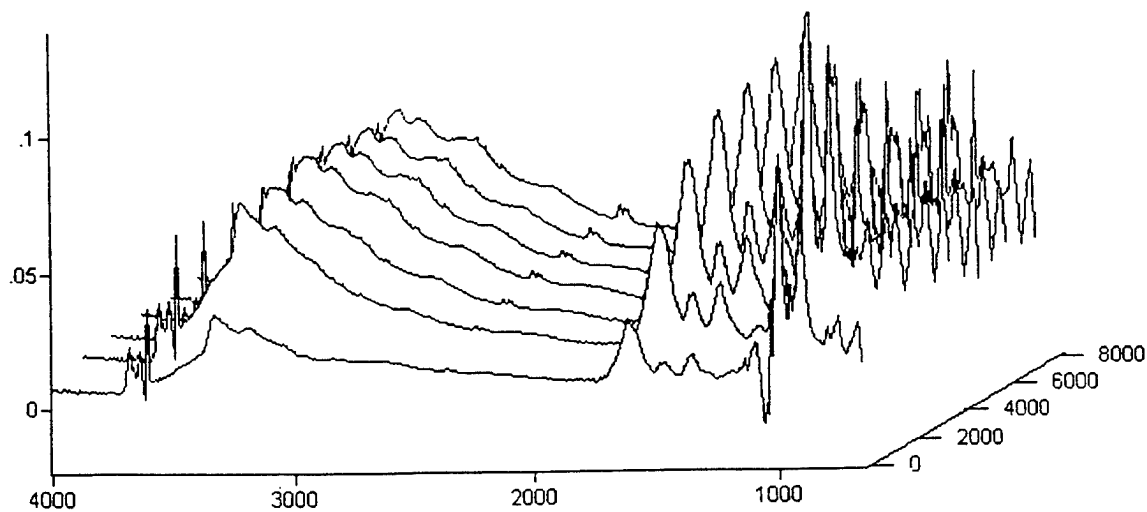
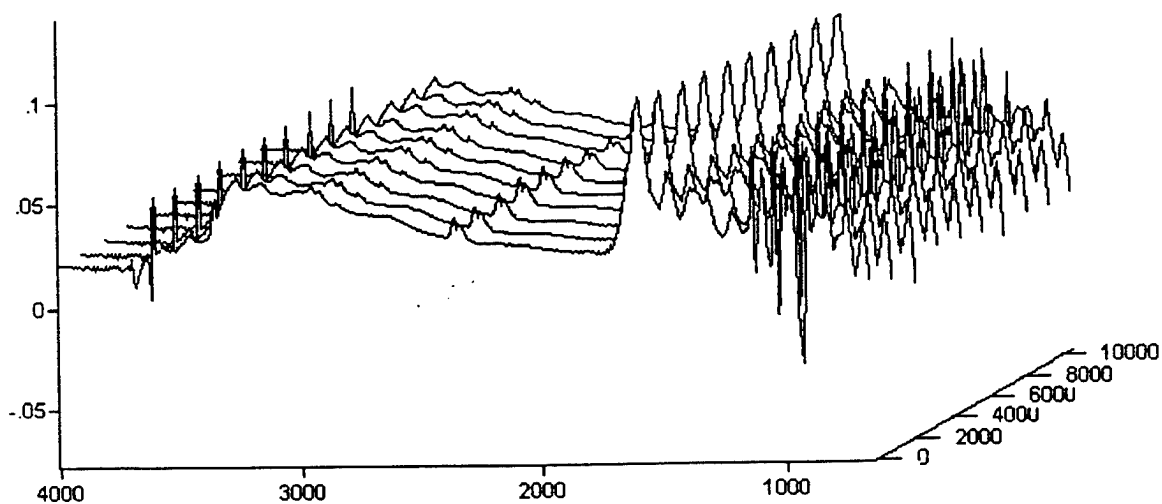


Figure 9.
ATR-FTIR spectrum of Georgia kaolin clay KGa-2 showing mineral band positions.



Time spectra of the interaction between hydrazine and KGa-1b. well-crystallized kaolin. Spectra taken at 20 minute intervals. Sample chamber remained closed.



Continuation of the timed spectra of hydrazine on KGa-1b.

Figure 10.

Spectra of the hydrazine-kaolin interaction with time.

intensity. These bands can be attributed to hydrazinium ion. It is likely that hydrazine occupies sites throughout the clay mineral, then reacts with the water associated with the clay mineral, in the interlamellar spaces. Evidence for this is provided by the band at 3617 cm^{-1} , which has been shifted to lower wavenumber as the hydrazine sorbs and interacts with a clay surface hydroxyl or oxygen group.

In identical experiments, poorly crystallized kaolin, KGa-2 was exposed to hydrazine in both the vapor state and in aqueous solution. Figure 11 shows the series of spectra of this kaolin clay exposed to hydrazine vapor over time. The reaction that occurs is exactly analogous to that found with KGa-1b. The spectra indicate that the bands seen, in this case at 3005 cm^{-1} , 2956 cm^{-1} , 2919 cm^{-1} , and 2850 cm^{-1} which appear to indicate the presence of hydrazinium ions as before. In this spectrum (not seen in the figure), an OH stretch at 3616 cm^{-1} also appears, but is of much lower intensity.

An experiment was conducted using an aqueous solution of hydrazine and a suspension of the KGa-1b. The spectra after mixing showed no sign of interaction. This could indicate that the hydrazine-KGa-1b interaction was not thermodynamically favorable. Unlike the spectra of KGa-1b, a hydrazine-KGa-2 kaolin interaction from the aqueous mixture could be detected (Figure 12). Spectrum B in this figure is the spectrum of the aqueous mixture dried onto the ATR cell. The NH stretches appear at 3318 cm^{-1} and 3192 cm^{-1} , as opposed to 3363 cm^{-1} , 3276 cm^{-1} and 3171 cm^{-1} from the vapor-deposition experiment. The aqueous adsorbate does show relatively large and complex bands near those we associate with the hydrazinium ion with bands at around 2979 cm^{-1} ,

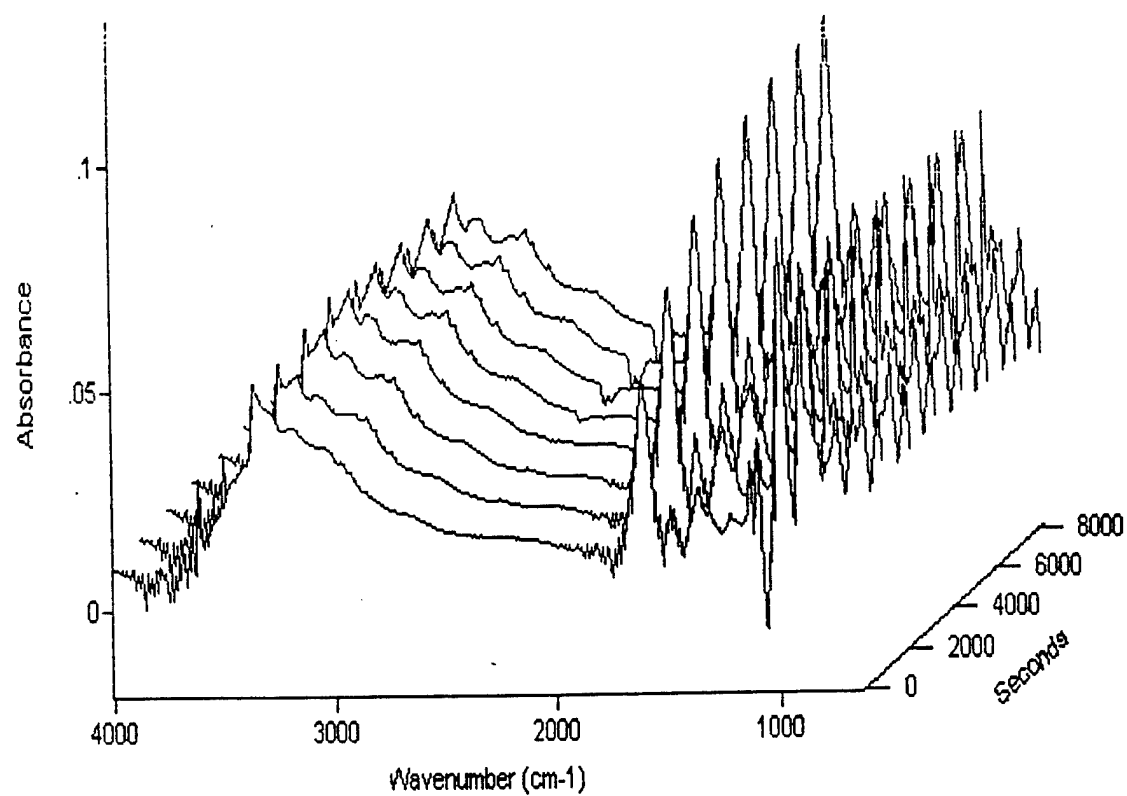


Figure 11.

Spectra of the interaction of hydrazine with poorly crystallized kaolin with time.
Spectra were taken every 20 minutes. Initial spectrum was taken at the 20 minute mark.

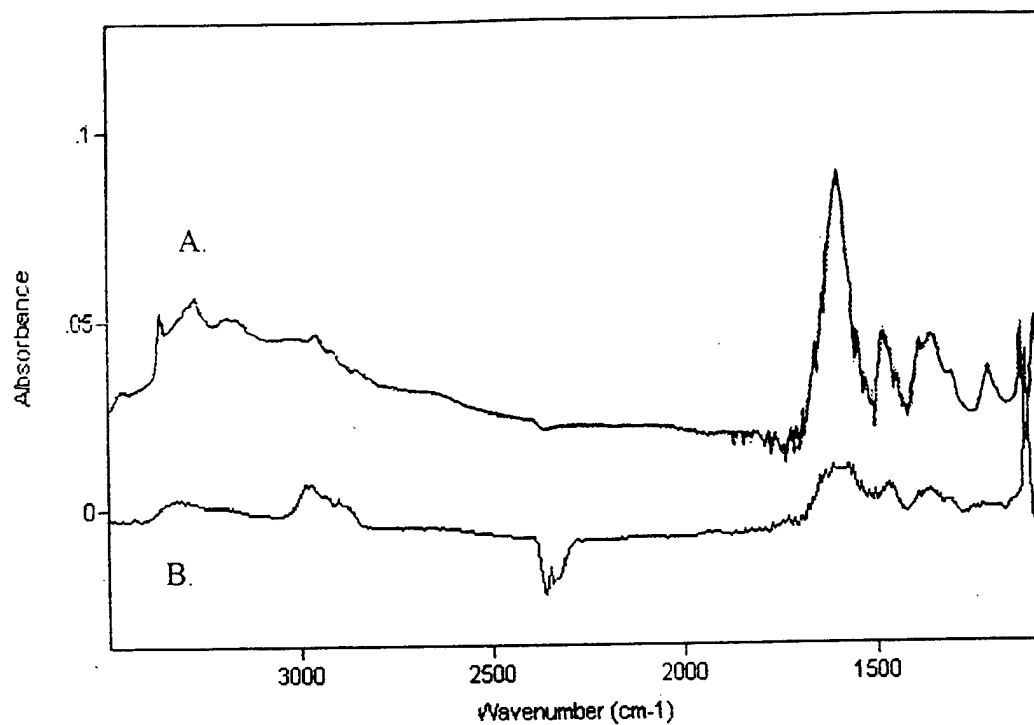


Figure 12.

Differences in vapor deposition of hydrazine and addition of hydrazine as an aqueous solution in KGa-2, poorly crystallized kaolin. Spectrum A. Is the hydrazine-kaolin complex made by vapor deposition, and B. Is made by an addition of aqueous solutions of the clay mineral and hydrazine. The major differences in these spectra are in the NH stretch region just above 3000 wavenumbers and the area just below 3000 wavenumbers.

2938 cm^{-1} , and 2882 cm^{-1} . The bands seen below 2000 cm^{-1} appear to be virtually identical in these spectra. The smectite clays, calcium and sodium montmorillonite were also subjected to the above experiments. When SWy-1, sodium montmorillonite was hydrated, it turned into a translucent gel, both in the presence of hydrated hydrazine, and without. Figure 13. shows spectra taken over time of the SWy-1-hydrazine complex made from the aqueous solution. As time passed, the sample was allowed to dry on the ATR cell. As the water spectrum decreases the spectrum of the hydrazine interaction appears. The lowest spectrum is of the sample after it has been heated. As the spectrum is not changed from the one above it, it is apparent that the sorbate is not heat-labile.

When spectra of the SWy-1-hydrazine sorbate deposited from an aqueous solution, is compared with that made by vapor deposition many differences can be seen in Figure 14. Both the vapor and liquid experiments show the interlamellar OH stretch at around 3616 cm^{-1} (in spectrum B for the vapor deposition, the band is folded downward in a subtraction artifact indicating that a background clay mineral band has shifted in response to the interaction). The NH stretches are also different, with the liquid sorbate absorptions occurring at 3356 cm^{-1} and 3300 cm^{-1} while those associated with the vapor occur at 3347 cm^{-1} and 2389 cm^{-1} . Even larger differences are seen in the NH_2 wags, found at 1604 cm^{-1} and 1357 cm^{-1} in the aqueous sorbate but at 1584 cm^{-1} and 1357 cm^{-1} for that formed from vapor deposition. Other bands between the two forms are also different suggesting a slightly different mechanism of interaction between the two sorbates. Both exhibit bands around the $-\text{NH}_3^+$ stretch band region, but both are of relatively small intensity. It appears that the interaction in this clay mineral also takes place in the interlamellar region and most

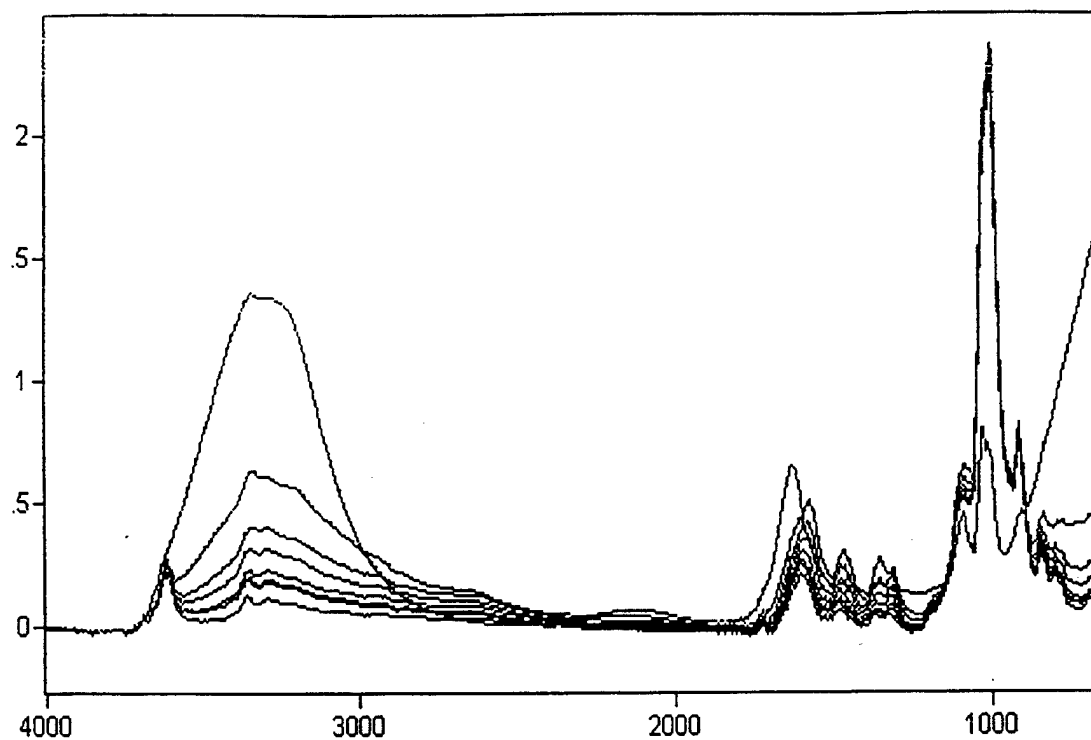


Figure 13.

Spectra of SWv-1, sodium montmorillonite with hydrazine added as an aqueous solution. The spectra illustrate the course of the loss of water from the sample on the ATR crystal.

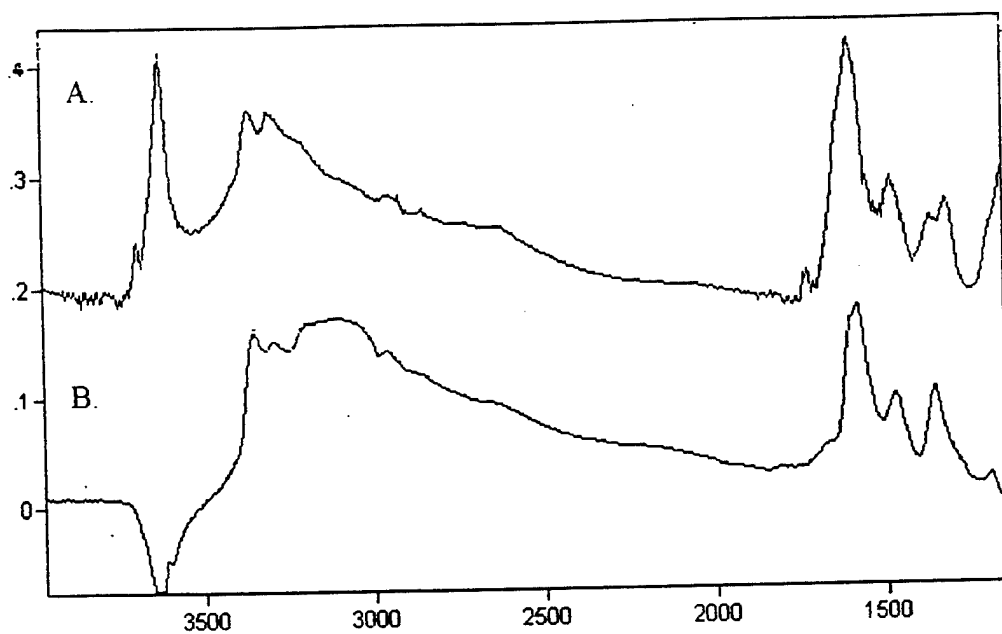


Figure 14.

Sodium montmorillonite. SWv-1 spectra of A. Deposition of hydrazine from an aqueous solution, and B. Deposition of hydrazine vapor on dry clay.

likely is a function of the hydrazinium ion bonding to waters of hydration around the interlamellar cations, or perhaps displacing them. In the case of vapor deposition, the hydrazinium interaction still takes place assuming that surface bound water is present on the clay, however another interaction with possibly the outer surfaces and edges of the clay is probable.

This same interesting difference between the complex formed by the two different methods is also seen with the calcium montmorillonite, SAz-1. Here the differences in the NH stretch region are more pronounced as seen in Figure 15. The NH stretch is 8 cm^{-1} higher in the vapor-derived sorbate versus that from aqueous solution. This is also true of the NH_2 wags at 1578 cm^{-1} and 1362 cm^{-1} (aqueous solution) as compared with 1609 cm^{-1} and 1374 cm^{-1} (vapor deposition). In this case, the bands associated with the hydrazinium ion are very small. A similar interaction as with the sodium montmorillonite is probable, but with the interaction most likely taking place with the hydration sphere around the interlamellar calcium.

G. OXIDATION OF DIMETHYLHYDRAZINES AS STUDIED BY GAS CHROMATOGRAPHY AND MASS SPECTROMETRY

In the initial experiments for the determination of dimethyl hydrazine decomposition products, various peaks were found to elute very close to the water solvent peak, but a few others were found to elute after the safety period demanded by the GC-MS detector safety control. These compounds were analyzed using the GC-MS, several of which were found to have quite high molecular masses. It is speculated that these compounds derived from presumably reactive intermediate compounds which have polymerized or condensed in the reaction vessel.

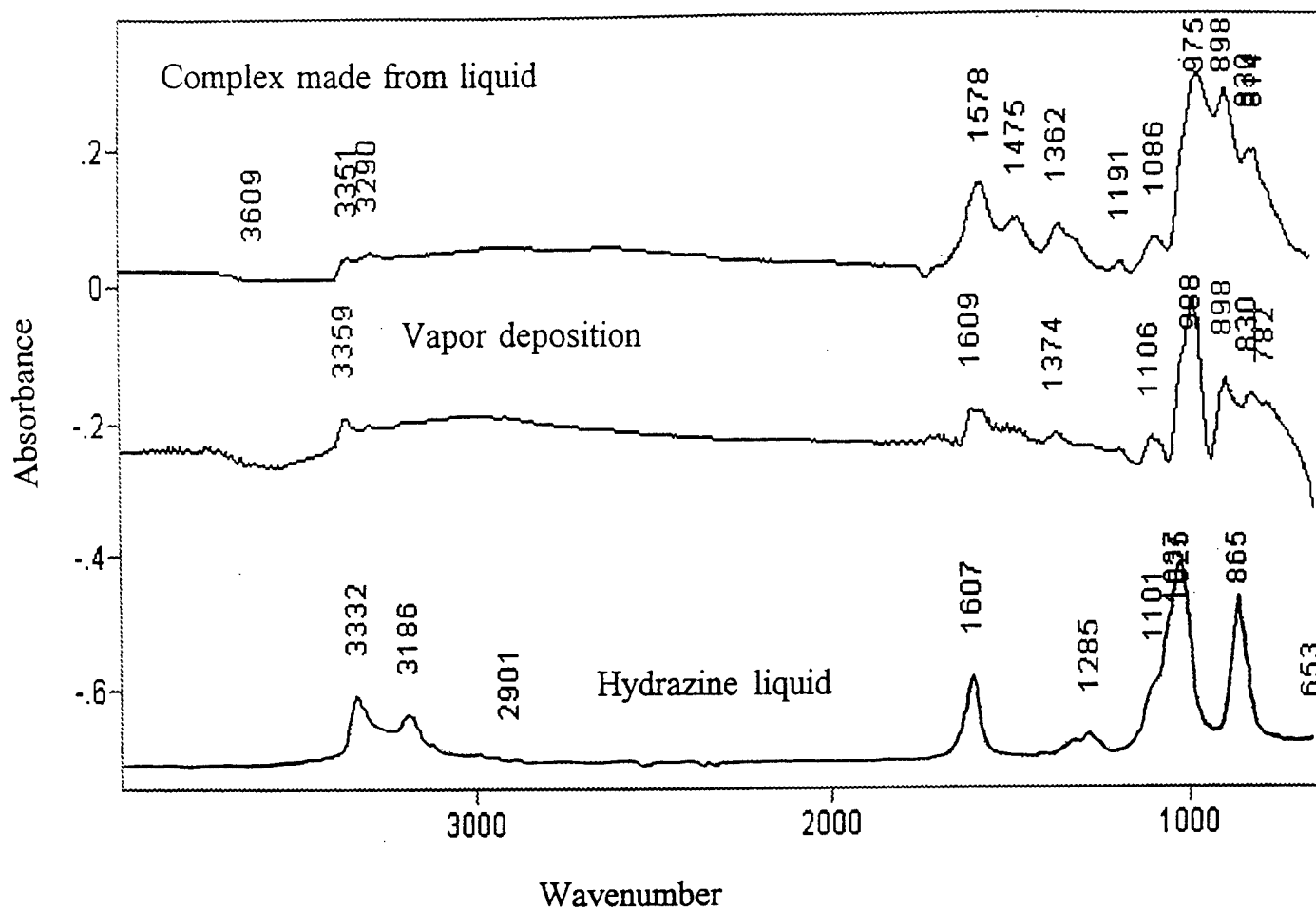
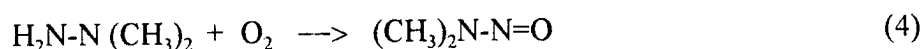


Figure 15.

Spectra of hydrazine-calcium montmorillonite prepared from an aqueous solution compared with that prepared by the deposition of hydrazine vapor on dry montmorillonite. The spectrum of pure liquid hydrazine appears at the bottom. Different shifts of the hydrazine bands may indicate a different interaction. The spectra of the calcium montmorillonite has been subtracted out in each case.

The analysis of several of the aqueous dimethyl hydrazine solution at around three hours reaction time revealed m/z peaks of 73 at about 10 minutes retention time on a 45° C column. This molecular mass corresponds to deprotonated dimethyl nitrosamine, a possible product of the oxidation of dimethyl nitrosamine as shown in Equation 4.



When the ether extraction followed by head space analysis was tried, again the dimethyl hydrazine peak and another peak which appears to be one of the more rapidly formed degradation products elute very close to the ether solvent peak as can be seen in Figure 16. We found that at 10 minutes into the reaction, the dimethyl hydrazine appears to elute at 1.455 min while the diethyl ether solvent eluted at 1.565 minutes. The peak at 1.935 is therefore the degradation compound. At this time, we were to try this method on the GC-MS where the detector protection controls were to be shut off such that even the diethyl ether solvent peak would go through the MS detector. However, the only way that this method could be done, even with head space vapor used instead of the actual liquid phase extract, was to eliminate the detector safety controls. The experiment was canceled when it was speculated that the solvent could destroy the mass detector, and that the small amount of compounds of interest that would pass the sample splitter might not be enough to detect even at the sensitivity of the MS.

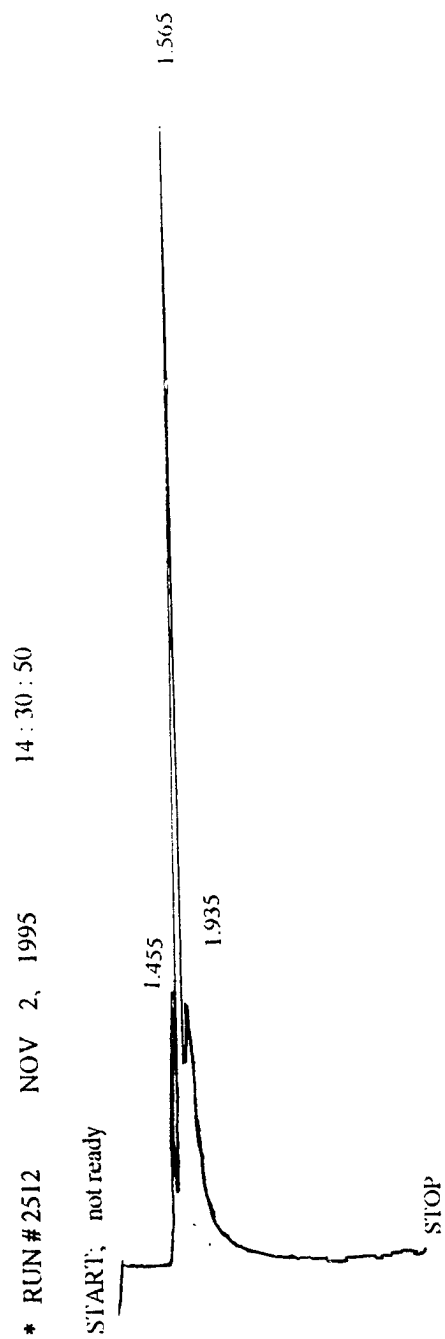


Figure 16.

Gas chromatogram of UDMH, decomposition products and the solvent.

H. BIOLOGICAL STUDIES

1. Effect of Hydrazine and Substituted Hydrazines on Microbial Respiration in Uncontaminated Soils

Hydrazine, methyl hydrazine and phenyl hydrazine were not inhibitory to normal microbial respiration in soil at concentrations of 5 and 50 mg/L. As may be seen in Figure 17, all of the treatments had similar slopes for CO₂ production (μmol CO₂/g soil). A comparison of the slopes with a one-way ANOVA yielded no significant differences among the three hydrazines or between the controls and hydrazine-amended soils ($\alpha = 0.05$, $p = 0.182$).

A second experiment was performed in which the same soils were amended with higher concentrations of the hydrazines (100 and 200 mg/L). The same protocol as for the lower concentrations was followed, and the results are summarized in Figure 18.

Unlike the strictly linear pattern of CO₂ production exhibited in soils exposed to the lower levels of hydrazines, soils amended with higher concentrations of hydrazine showed a more logarithmic pattern of CO₂ evolution. The reason for this difference is unknown. A statistical comparison of total CO₂ produced among treatments using a one-way ANOVA again yielded no significant differences among the three hydrazines or between the controls and hydrazine-amended soils ($\alpha = 0.05$, $p = 0.256$).

These results are probably easily explained by what we now know to be the reaction products formed in soils. In other words, hydrazine and the substituted hydrazines added to the soils in the

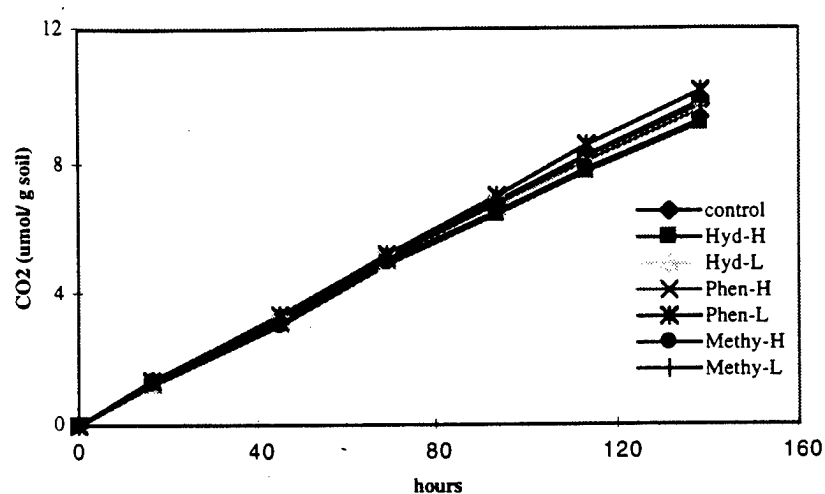


Figure 17.

Production of CO₂ by soil microorganisms with 5 or 50 mg/L of hydrazine, methyl hydrazine and phenyl hydrazine or no added hydrazines (controls). The data plotted represent the mean results of triplicate biometer flasks. L = 5 mg/L; H = 50 mg/L.

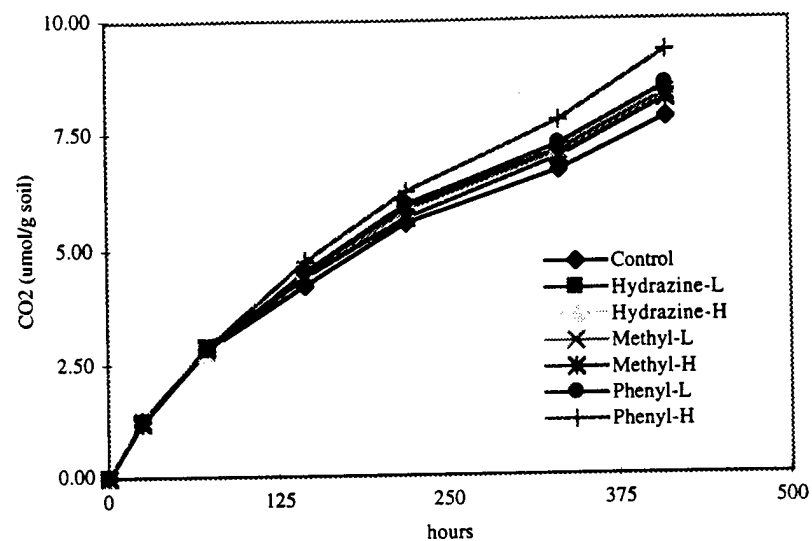


Figure 18.

Production of CO₂ by soil microorganisms with 100 and 200 mg/L of hydrazine, methyl hydrazine and phenyl hydrazine or no added hydrazines (controls). The data plotted represent the mean results of triplicate biometer flasks. L = 100 mg/L; H = 200 mg/L.

biometer flasks were rapidly converted to harmless end products (e.g., N_2 and some carbon fragments).

Hydrazine levels were not monitored during these experiments, but it is likely that the soil microbial community was not exposed to the hydrazines by virtue of their rapid autoxidation.

2. Effect of Hydrazine on Bacterial Sulfate Reduction

Anaerobic conditions were maintained throughout the duration of these experiments, as evidenced by the colorless status of the redox indicator (resazurin) used in the culture medium. Sulfate concentrations in the cultures were followed accurately. In all cases, the standard deviation of the four replicate values in each treatment was less than $0.05 C/C_0$ at each time interval. As expected, sulfate reduction by *D. desulfuricans* commenced rapidly in the unamended control cultures (see Figure 19). But an obvious lag time of 6 days before the onset of sulfate reduction was observed in the culture containing the lowest concentration of hydrazine (5 mg/L). Higher concentrations of hydrazine (50 and 100 mg/L) completely inhibited sulfate reduction by *D. desulfuricans*.

Under oxygen-free conditions, we see a pronounced toxicity of hydrazine concentrations to this particular sulfate-reducing bacterium. The greater toxicity of hydrazine to anaerobes is probably related to its greater stability under low redox conditions.

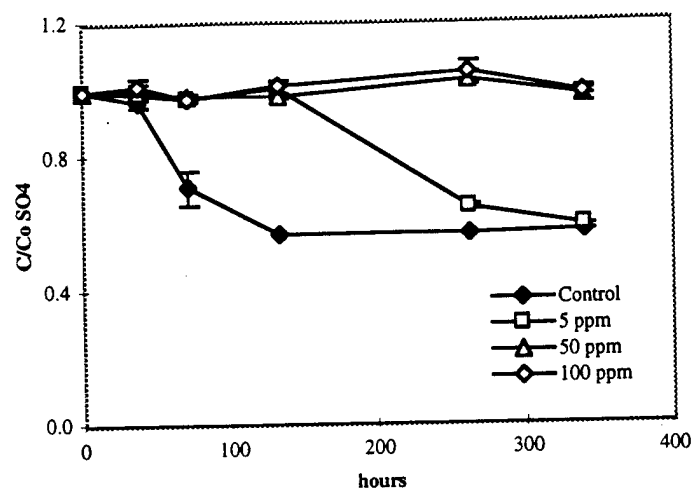


Figure 19.

Hydrazine inhibition of sulfate reduction in the *D. desulfuricans*. Data represent the mean sulfate values obtained from quadruplicate microcosms.

SECTION IV

CONCLUSIONS

The isotherm and autoxidation data show that about 60% of the hydrazine is consumed by aerial oxidation of the control whereas only about 20% disappears for the hematite system. The nature of this "protection" from autoxidation is not clear, but is of great importance with regard to fate and transport. At least two mechanisms are likely, (1) adsorption as hydrazinium (either 1^+ or 2^+ ions, see the ATR-FTIR results) inhibits reaction with oxygen, and, (2) aggregation of colloids induced by hydrazine adsorption which results in trapping hydrazinium in the internal structure of the aggregate leading to lack of diffusional access to O_2 . Note that our procedure is effective at measuring both hydrazine associated with the colloid (or aggregate) and that which is merely dissolved.

Given the ubiquitous distribution of colloidal iron minerals in groundwater, especially in the western states, either of the above mechanisms have profound consequences for fate and transport of hydrazines in groundwater, and their eventual distribution in soils. For example, adsorption to iron oxides (in general) could result in inhibition of autoxidation as a natural mitigating factor and to *enhanced transport* due to the colloid acting as a vector. In the case of aggregation, settling of the aggregates into the anoxic zone of aquatic environments could yield *increased residence times* in the environment, and in fact make hydrazines available in large quantities to anaerobic iron bacteria.

It was found that in the case of hydrazine the interaction with hematite appears to be through the hydrazinium ion and is most likely an electrostatic interaction with a surface hydroxide, or with a hydration sphere water on the hematite colloid. From the ATR-FTIR spectral analysis, the hydrazine interaction was observed to change with time, starting with what is apparently a hydrogen bonding situation, followed by an abstraction of what is most probably a water molecule hydrogen bonded to a hematite surface oxygen (hydration sphere water). This appeared to be followed by the stronger electrostatic interaction. At long contact periods, it appears that the hematite structure may be altered through this interaction. It was also found that there is little difference between the interaction prepared in solution and that prepared by vapor deposition, and that the interaction appears stable to heating.

Methyl hydrazine reacts to form a stable complex in a similar fashion to that of hydrazine. In the first few minutes, the spectrum changes with time rapidly but without the shifting in the NH stretch region. The spectrum rapidly stabilizes to a final unchanging form suggesting that a strong, final interaction is formed, which is not labile to heat, and does not evolve over a period of time as is the case with hydrazine. From changes in the CH stretch region, inconclusive evidence may suggest that an electrostatic interaction involving methyl hydrazinium ion occurs.

Our oxidation experiments followed by gas chromatography and mass spectrometry suggest that during autoxidation, dimethyl hydrazine forms dimethyl nitrosamine and unknown higher molecular weight products, possibly due to polymerization. These data indicate that nitrosamines, known for their toxicity and mutagenicity, may be let into the environment during autoxidation.

Clay minerals were found to interact with, and with the possible exception of one of the kaolin clays, to form stable interactions with hydrazine. Due to the complex nature of the clay mineral structures, hydrazine was found to interact differently with the clay minerals depending on whether the mode of interaction was from the vapor state or whether the hydrazine was in an aqueous solution. It was found that the interactions formed by both methods were stable to heat, but further studies will be required to determine if there is a difference in the strength of the respective interactions. If the interactions are strong, clay minerals with sorbed hydrazines could provide a vector for the distribution of hydrazines in the environment, both by water, and in the dry state by wind. It was also demonstrated that FTIR as a method for the investigation of interactions between pollutant compounds and individual soil components is a powerful and useful tool.

Experiments aimed at assessing the toxicity of hydrazine and substituted hydrazines to soil microflora, not in the presence of hematite or clay minerals, suggest that autoxidation reactions are rapid such that the microbes were probably only exposed to harmless end products. There is likewise no evidence of stimulation of microbial activity. Anaerobic toxicity assays, on the other hand, suggest that hydrazine is toxic to sulfate-reducing bacteria.

Probably the greatest environmental concern of hydrazine-based compounds is related to their high aqueous solubility and corresponding potential to rapidly leach from surface soils to ground water. Below the soil surface, aquifers are often oxygen limited or anoxic, and hydrazine may be stable under these conditions. Once such compounds pass below the soil surface, their attenuation may be largely dictated by anaerobic microorganisms. Their high solubility, apparent stability under

anaerobic conditions and inhibition of microbial activity all favor persistence of hydrazines in anaerobic environments. In soils, however, their rapid reactivity with metals and clays may render them harmless long before they ever leach to the subsurface.

REFERENCES

1. A. R. Slonim, J. B. Gisclard, (1976). *Bulletin of Environmental Contamination & Toxicology*, 16, 3, 301-309.
2. Moliner, A., Street, J. (1989). "Decomposition of Hydrazine in Aqueous Solutions." *J. Environ. Qual.* 18:483-487.
3. Zhong, Y., Lim, P., (1989). "The copper-catalyzed Redox Reaction between Aqueous Hydrogen Peroxide and Hydrazine. 1. New Experimental Results and Observations." *J. Am. Chem. Soc.* 111, 8398-8404.
4. Coyne, L., Mariner, R., Rice, A., (1991). "Air Oxidation of Hydrazine. 1. Reaction Kinetics on Natural Kaolinites, Halloysites, and Model Substituent Layers with Varying Iron and Titanium Oxide and O-Center Contents." *Langmuir*, 7, 1660-1674.
5. Coyne, L., Summers, D., (1991). "Surface Activation of Air Oxidation of Hydrazine on Kaolinite. 2. Consideration of Oxidizing/Reducing Entities in Relationship to Other Compositional, Structural, and Energetic Factors." *Langmuir*, 7, 1675-1688.
6. Schmidt, E. W. *Hydrazine and its Derivatives. Preparation, Properties, Applications*, Wiley- Interscience, NY, 1984 p 344-349.
7. Funai, I. A., Blesa, M. A., Olabe, J. A., (1989). "Hydrazine Autoxidation in Solution: Catalysis by Pentacyanoferrate(II)", *Polyhedron*, 8,4,419-426.
8. Smith, M. R., Keys, R. L., Hillhouse, G. L., (1989). "Oxidation of Methylhydrazine at a Metal Center. Stereoselective Synthesis of cis-Methyldiazene, $\text{NH}^+\text{N}(\text{CH}_3)$, *J. Am. Chem. Soc.* 111, 8312- 8314.

9. Loper, G. L., "Gas phase kinetic study air oxidation of UDMH" *Proceedings of the Conference on Environmental Chemistry of Hydrazine Fuels*, Tyndall AFB, 13 September 1977, CEEDO-TR-78-14, p 129-160.
10. Moliner, A., Street, J. (1989). "Decomposition of Hydrazine in Aqueous Solutions." *J. Environ. Qual.* 18:483-487.
11. Moliner, A., Street, J., (1989). "Interactions of Hydrazine with Clays and Soils", *J. Environ. Qual.* 18: 487-791.
12. Miller, T. L. and M. J. Wolin. (1974). "A serum bottle modification of the Hungate technique for cultivating obligate anaerobes." *Appl. Microbiol.* 27: 985-987.
13. Widdel, F. . *Anaerober Abbau von Fettsauren and Benzosaure durch neu isolierte Arten sulfat-reduzierender Bakterien. (Anaerobic Degradation of Fatty Acids and Benzoic Acid by Newly Isolated Types of Sulfate-Reducing Bacteria)*. Doctoral Dissertation, Georg-August-Universitat, Gottingen, 1980.
14. Tipton, T., Person, W., Kubulat, K., Vala, M., Stone, D., *A Matrix-Isolation FT-IR study of hydrazine. p.138-153. In D.A. Stone and F.L. Wiseman (ed) The 3rd Conf. Environ. Chem. of Hydrazine Fuels*, Panama City, FL. 15-17 Sept. 1987. ESL-TR-87-74. Eng. and Serv. Lab., Tyndall AFB, FL.
15. Sulbha, A., Gupta, V., (1988). "Spectrophotometric determination of trace amounts of hydrazine in polluted water." *Analyst*, 113, 1481-1483.
16. Penners, N., Koopal, L., (1986). "Preparation and optical properties of homodisperse haematite hydrosols." *Colloids and Surfaces*, 19, 337-349.

17. Bowen, J., Powers, C., Ratcliffe, A., Rockley, M., Hounslow, A., (1988). "Fourier transform infrared and Raman spectra of dimethyl methylphosphonate adsorbed on montmorillonite." *Environ. Sci. Technol.* 22, 1178-1181.
18. Brett, C. M. A., Brett, A. M. O., *Electrochemistry: Principles, Methods, and Applications*. Oxford University Press, Oxford, 1993, p55.
19. Durig, J. R., Bush, S. F., Mercer, E. E., (1966). "Vibrational spectrum of hydrazine-d4 and a Raman study of hydrogen bonding in hydrazine." *J. Chem. Phys.*, 44, 11, 4238-4247.
20. Glavic, P., Hadzi, D., (1972). "The Infrared Spectrum of hydrazinium (+1) Fluoride", "*Spectrochimica Acta*", 28A, 1063-1067. And Patil, K. C., Vittal, J. P., (1982). "Synthesis and characterization of a new sulphate derative of hydrazine $N_2H_5HSO_4$ ", *J. Chem. Soc. Dalton Trans.* 2291.
21. Decius, J. C., Pearson, D. P., (1953). "The infrared absorption of crystalline and liquid hydrazine monochloride and monobromide," *J. Am. Chem. Soc.* 75, 2436-2439.
22. Snyder, R. G., Decius, J. C., (1959). "The infrared spectra of $N_2H_6Cl_2$ and $N_2H_6F_2$," *Spectrochimica Acta*, 13, 280-290.
23. Theng, B. K. G., *Formation and Properties of Clay-Polymer Complexes*. Elsevier Scientific Publishing Company, New York, (1979).

TR Mailing List for EQPI

HQ AETC/CEV
Bldg 661
73 Main Circle
Randolph AFB TX 78150-4549

DTIC
Attn: DTIC-OCF
Bldg 5
Cameron Station
Alexandria VA 22304-6145

HQ AFRES/CEV
155 2nd Street
Robins AFB GA 31098-1635

HQ USAFA/DFSEL
2354 Fairchild Drive, Suite 3A15
USAF Academy CO 80840-6214

HQ PACAF/CEV
25 E Street, Suite D-302
Hickam AFB HI 96853-5412

HQ USAF/CEV
115 Brookley Ave, Suite 1
Bolling AFB DC 20332-5106

AUL/LSD
600 Chennault Circle, Bldg 1405
Maxwell AFB AL 36112-6424

HQ AFMC/CEV
4225 Logistics Ave
Wright-Patterson AFB OH 45433-5006

WL/POTC
1950 5th Street, Bldg 18
Wright-Patterson AFB OH 45433-7251

USAE Waterways Experiment Station
Attn: WES EE-S/John Cullinane
PO Box 631
Vicksburg MS 39180-0631

HQ AFSPACECOM/CEV
150 Vandenberg Street, Suite 1105
Peterson AFB CO 80914-4150

Director
US EPA Robert S Kerr Environmental
Research Lab
PO Box 1198
Ada OK 74821-1198

Cathy Vogel (10)
AL/EQW-OL
139 Barnes Drive, Suite 2
Tyndall AFB FL 32403-5323

Allen Tool
US Army COE
Kansas City District
601 E 12th Street
Kansas City MS 64106-2896

HQ USAFE/CEV
Unit 3050, Box 10
APO AE 09094-3050

HQ AMC/CEV
507 A Street
Scott AFB IL 62225-5022

ANGRC/CEV
3500 Setchet Ave, Bldg 3500
Andrews AFB MD 20331-5157

WL-MNOI - Tech Library
203 W Eglin Blvd, Suite 300
Eglin AFB FL 32542-6843

AL/OEBE
2402 E Drive
Brooks AFB TX 78235-5114

AFIT/CE
2950 P Street
Wright-Patterson AFB OH 45433-7765

AFIT/LSM
2950 P Street
Wright-Patterson AFB OH 45433-7765

Environmental Quality Division
NAVFAC Code 112
200 Stovall Street
Alexandria VA 22332

HQ ACC/CEV
129 Andrews Street, Suite 346
Langley AFB VA 23665-2769

US Army Research Office
PO Box 12211
Research Triangle Park NC 27709

Dept of the Army
Commander
CERL
PO Box 4005
Champaign IL 61824-4005

Naval Facilities Engineering
Service Center
Code ESC40
5660 Center Drive
Port Hueneme CA 93043-4328

DET 3
Unit 5213
AL
APO AP 96318-5213

AFCEE/EST
2504D Drive, Suite 3
Brooks AFB TX 78235-5103

NGB/CE
2500 Army Pentagon, RM 2D369
Washington DC 20331-2500

Bruce C. Alleman, PhD (15)
Battelle Memorial Instititue
505 King Avenue
Columbus OH 43201-2693